Assessing 3D metric data of Digital Surface Models for extracting archaeological data from archive stereo-aerial photographs

Heather Papworth (corresponding author)[a], Andrew Ford[b], Kate Welham[a], and David Thackray[c]

[a]Department of Archaeology, Anthropology & Forensic Science

[b]Department of Life & Environmental Sciences

[c]ICOMOS UK

Bournemouth University

Faculty of Science and Technology

Talbot Campus, Fern Barrow

Poole, Dorset. BH12 5BB

Email: h.e.papworth@gmail.com

Abstract

Archaeological remains are under increasing threat of attrition from natural processes and the continued mechanisation of anthropogenic activities. This research analyses the ability of digital photogrammetry software to reconstruct extant, damaged, and destroyed archaeological earthworks from archive stereo-aerial photographs. Case studies of Flower's Barrow and Eggardon hillforts, both situated in Dorset, UK, are examined using a range of imagery dating from the 1940s to 2010. Specialist photogrammetric software SocetGXP® is used to extract digital surface models, and the results compared with airborne and terrestrial laser scanning data to assess their accuracy. Global summary statistics and spatial autocorrelation techniques are used to examine error scales and distributions. Extracted earthwork profiles are compared to both current and historical surveys of each study site. The results demonstrate that metric information relating to earthwork form can be successfully obtained from archival photography. In some instances, these data out-perform airborne laser scanning in the provision of digital surface models with minimal error. The role of archival photography in regaining metric data from upstanding archaeology and the consequent place for this approach to impact heritage management strategies is demonstrated.

Keywords

Digital photogrammetry; archaeology; archive stereo-photographs; earthworks; reconstruction; digital surface models; laser scanning.

1. Introduction

Archaeological sites are subject to substantive on going decay and damage caused by a variety of both natural and human behaviours (Rowley and Wood 2008). Factors such as increased storm rates and sea-level rise, and the sharp growth in the efficiency, rate and scale at which many anthropogenic activities occur within the UK landscape are a pressing issue for many regions (Oxford Archaeology 2002; Murphy et al. 2009). Subsequently it has been estimated that, of the 600,000 sites in England, one has been lost per day since 1945 (Darvill and Fulton 1998). This equates to a projected disappearance rate of at least 25,000 sites over the past 70 years, and nowhere is this more apparent than in the tangible loss and damage of earthwork features.

In an attempt to mitigate this loss a number of conservation charters exist that advocate recording archaeological sites before they are destroyed (Bassegoda-Nonell et al. 1964; ICOMOS General Assembly 1996), but the reality of achieving this ideal is an immense challenge. Within the UK alone the high density and sheer variety of monuments mean that there are inevitably large numbers of sites where damage or destruction has occurred, and the level of recording undertaken has been minimal, or in some extreme cases non-existent. The ability to utilise archive data from the periods subsequent to the disappearance of such sites to reconstruct what previously existed would be of significant benefit, not only for the understanding of these monuments but, just as importantly, to inform the conservation, management and interpretation of our heritage assets in the future.

Fortunately, an archive containing these data does exist. In the UK, stereo-aerial photographs (SAPs) have been gathered regularly, and on a large scale, since the 1940s. These images hold within them the potential for landscape reconstruction. Three-dimensional (3D) data can be extracted using digital photogrammetry methods to create digital surface models (DSMs); an approach that has already been successfully used in the geomorphology and surveying disciplines to assess terrain change over time (Chandler 1989, Adams and Chandler 2002, Walstra et al. 2004, Walstra 2006, Miller et al. 2008, Aguilar et al. 2013). In contrast, although archaeologists have been utilising aerial photography for over a century and are experts in prospecting for and mapping earthwork features from them in two-dimensions (Wilson 2000, p.16; Barber 2011, p.215), very few have acknowledged the inherent 3D properties of SAPs (Verhoeven et al. 2012) beyond the use of stereoscopes.

This research employs qualitative and quantitative methods to assess the ability of archive SAPs to reconstruct extant, damaged and destroyed earthworks. Two case study sites are used to compare the results obtained from digital surface models created from a range of SAPs to those achieved via modern metric survey techniques commonly used in the archaeology and heritage sectors: global navigation satellite systems (GNSS), and terrestrial and airborne laser scanners. The utility of these data when compared to both objective (metric) and interpretative (such as hachure plans) survey is discussed (Bowden and McOmish 2012; Blake 2014).

2. Data and Methods

2.1 Field Site Selection

The field study sites of Flower’s Barrow and Eggardon Iron Age hillforts (Figures 1 and 2) were selected as they both contain a mixture of subtle and pronounced earthworks, some of which are well preserved and stable whilst others have been damaged or destroyed via natural or anthropogenic agents.

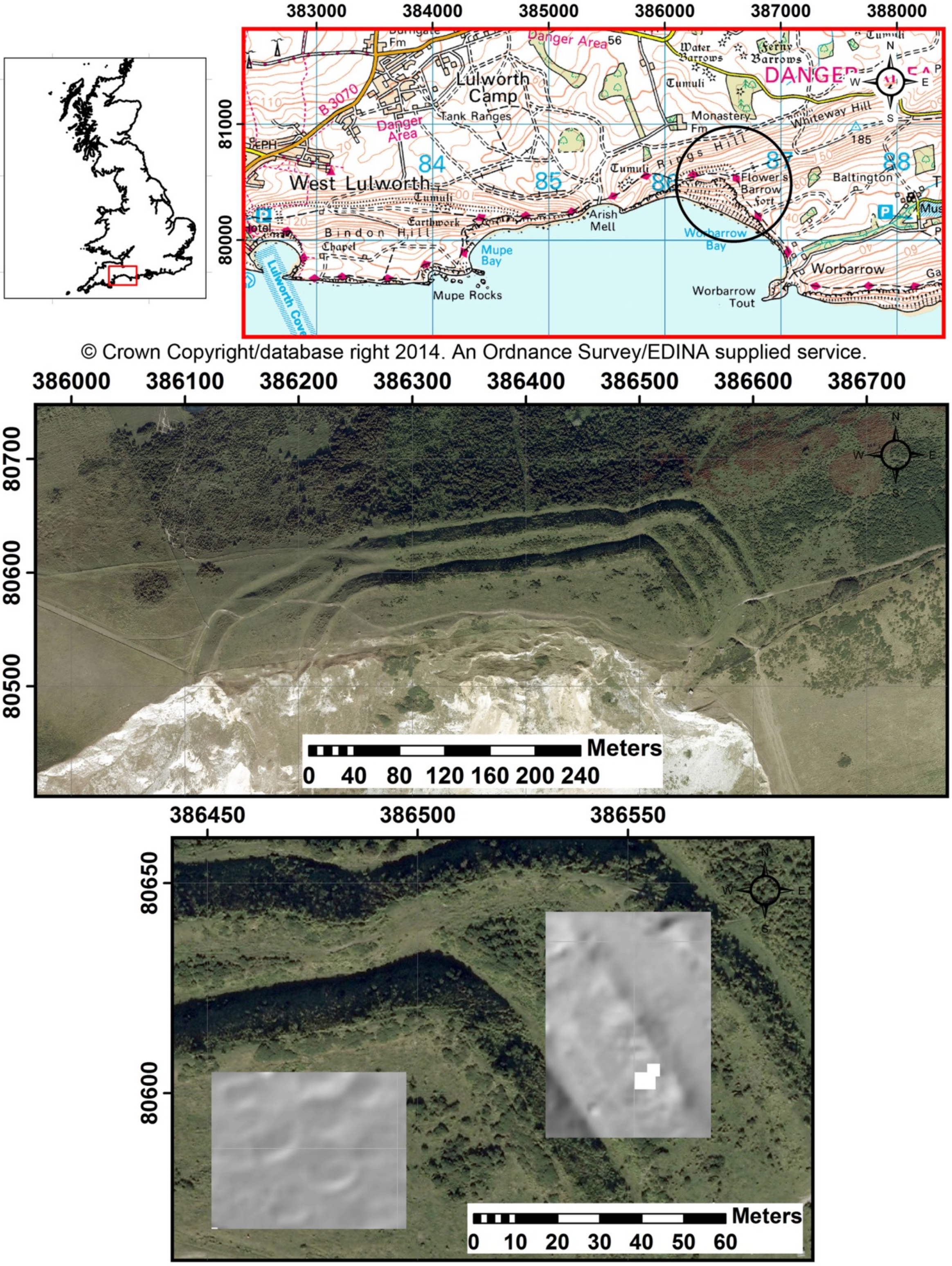

Figure 1: Location of Flower's Barrow hillfort within the United Kingdom including an orthophotograph of the site and examples of earthworks within the hillfort (Bottom Left) Occupation Platforms and (Bottom Right) a linear annex.

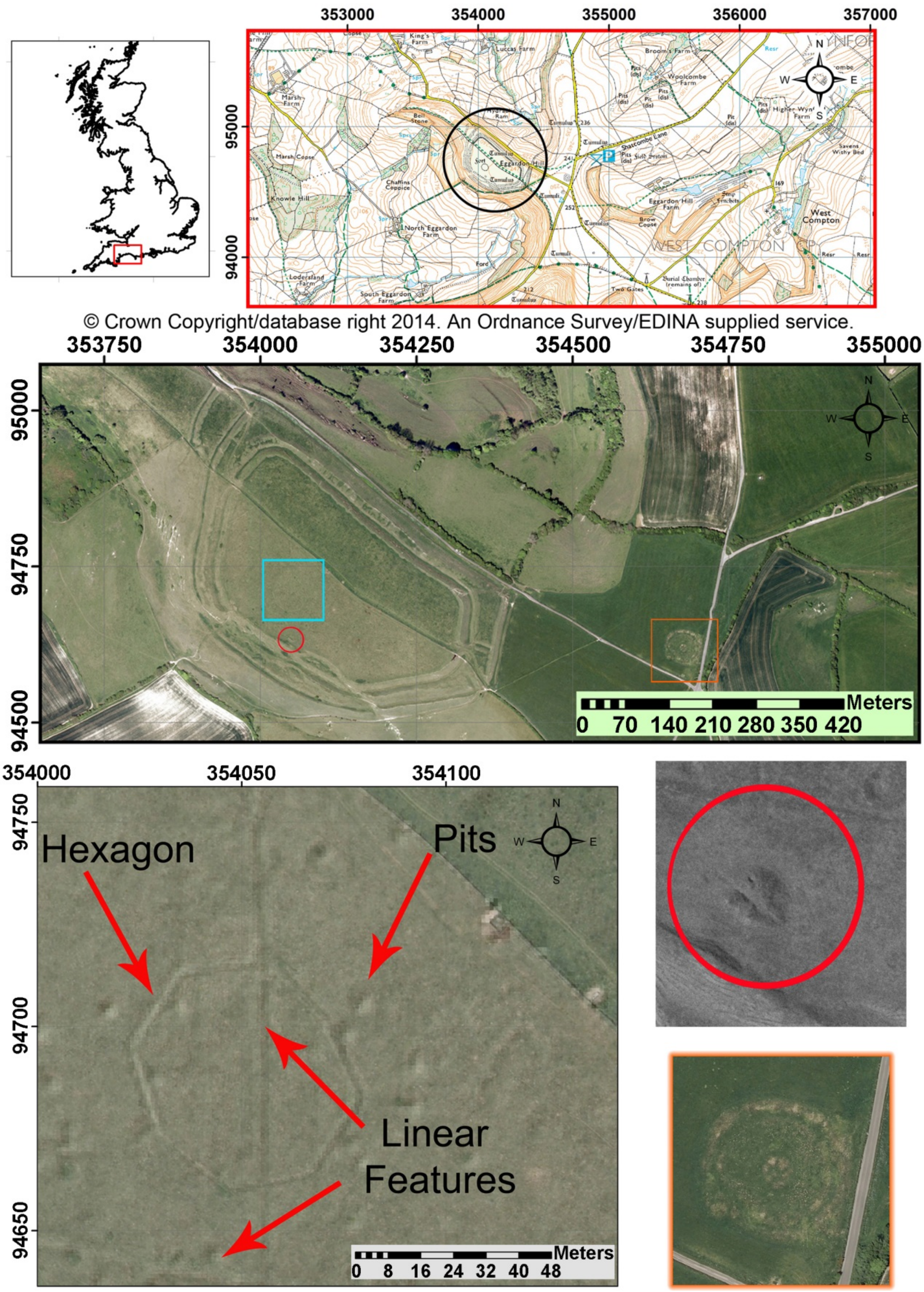

Figure 2: Location of Eggardon within the United Kingdom including an orthophotograph of the site and examples of earthworks within the hillfort including (Bottom Left) linear features and pits, (Bottom Upper Right) damaged barrow and (Bottom Lower Right) henge monument.

Coverage of each area with archive SAPs devoid of cloud cover and with suitable stereo-overlap is available, with a range of imagery for each decade from the 1940s to the present day. Flower's Barrow is situated on Defence Estates land and the site is only accessible to the public on weekends and during major school holidays, thus footfall is limited. A condition assessment completed by Wessex Archaeology (2001) identified the hillfort and its environs as being in good condition, although the southern ramparts have been lost to cliff erosion since construction. The terrestrial hinterland is, however, stable. Eggardon is unique in that the northern half of the hillfort interior has been damaged by irregular ploughing since the 1940s, whilst the southern half is separated by a fence denoting the parish boundary and has remained in the custody of the National Trust, facilitating its preservation.

2.1.1 Baseline Data Collection

A baseline reference metric survey was collected at each site using a Leica C10 terrestrial laser scanner (TLS) whose station locations were ascertained using a Leica Viva GNSS. A sub-10cm point cloud was achieved within the hillfort at each site, with the Mean Absolute Error for the dataset at Flowers Barrow calculated by Leica Cyclone as 0.011m and at Eggardon Hillfort as 0.014m. The TLS point density as created at each field site is shown in Figure 3.

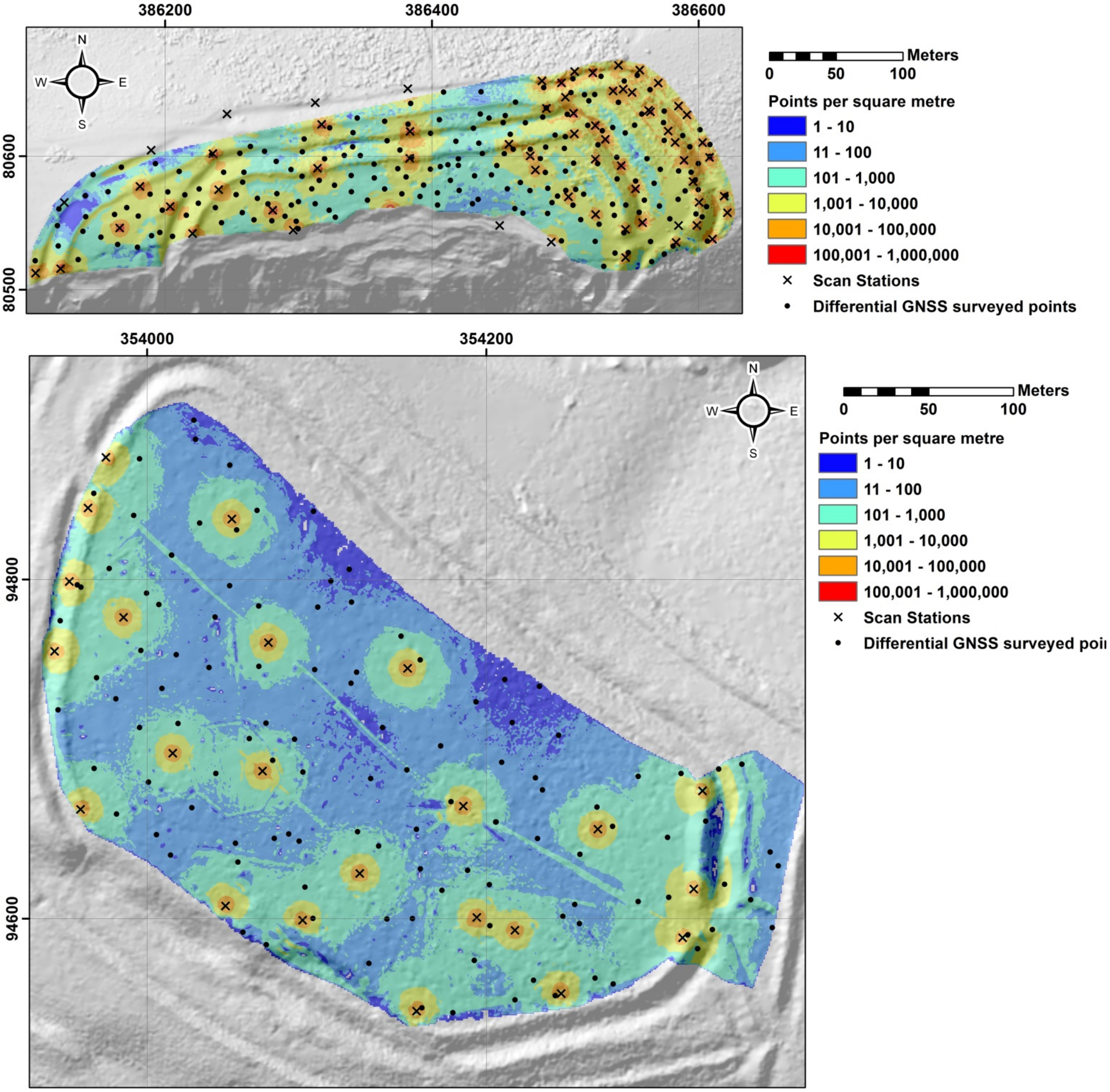

Figure 3: Diagrams illustrating TLS point density created at Flowers Barrow (above) and Eggardon Hillfort (below).

To identify systematic errors in the TLS dataset prior to undertaking analysis with it, a number of random points were collected across each field site using a Leica Viva GNSS. The residual differences between TLS and GNSS elevation values are illustrated in Figure 4.

20cm, with very few values exceeding this figure. The graphs in Figure 5 illustrate the lack of correlation between residual elevation values between the TLS and GNSS in relation to the proximity of measurements to the scanner and as a function of TLS point density. Subsequently it can be said that neither the proximity of the TLS data to the scanner or the point density of the data influences error in the TLS data.

2.2. Archive Stereo-Aerial Photographs and Airborne Laser Scanning

Archive SAPs for both sites were obtained from the National Monuments Record (NMR) in Swindon, Bournemouth University (BU), and Dorset County Council (DCC) (Table 1).

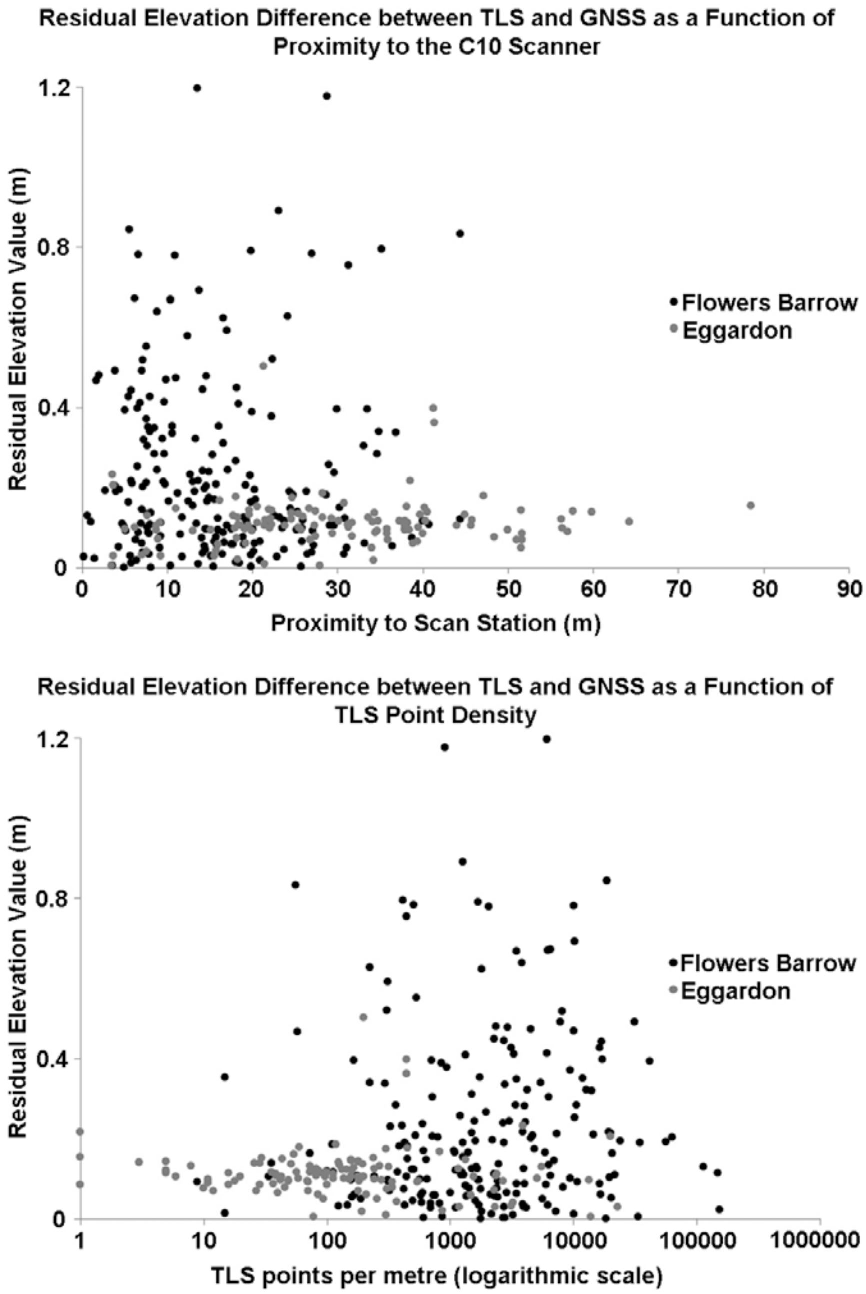

Figure 5: Scatter plots demonstrating the lack of a relationship between residual elevation values when examining these as a function of proximity to the location of the C10 TLS (above) and as a function of TLS point density (below).

Flower's Barrow Archive Stereo-Aerial Photographs

Date Flown	Archive/ Creator	Scale	Focal Length (mm)	Flying Height (m)	Ground Sample Distance (m)	Image Type (Verticals)	Format (cm)	*Original Media
March 1945	NMR/RAF	1:10500	203.2	2133.6	0.110	B&W	12.7x12.7	Negative
August 1968	NMR/RAF	1:10000	152.4	1524	0.118	B&W	23x23	Negative
June 1972	BU/J.A.Storey	1:12000	151.85	1822.2	0.132	B&W	23x23	Print
April 1982	NMR/OS	1:8000	304.8	2438.4	0.081	B&W	23x23	Negative
June 1986	DCC/ C.E.G.B.Winfrith	1:12000	153.05	1836.6	0.135	B&W	23x23	Print
1997	DCC/ C.E.G.B.Winfrith	1:10000	153.15	1531.5	0.114	Colour	23x23	Print
Sept. 2009	GetMapping Ltd.	-	100.5	-	0.150	Colour	10.39x6.78	Digital

Eggardon hillfort Archive Stereo-Aerial Photographs

Date Flown	Archive/ Creator	Scale	Focal Length (mm)	Flying Height (m)	Ground Sample Distance (m)	Image Type (Verticals)	Format (cm)	*Original Media
January 1948	NMR/RAF	1:10000	508	5029.2	0.104	B&W	20.95x19.05	Negative
March 1948	NMR/RAF	1:10000	508	5029.2	0.114	B&W	20.95x19.05	Negative
April 1969	NMR/OS	1:7500	304.8	2286	0.072	B&W	23x23	Negative
October 1972	DCC/J.A.Story	1:12000	151.85	1822.2	0.122	B&W	23x23	Print
April 1984	NMR/OS	1:8000	304.8	2438.4	0.078	B&W	23x23	Negative
July 1989	NMR/OS	1:8200	304.8	2499.4	0.084	B&W	23x23	Negative
Sept. 1997	DCC/ NRSC Airphoto Group	1:10000	153.15	1531.5	0.104	Colour	23x23	Print
2010	GetMapping Ltd.	-	100.5	-	0.150	Colour	10.39x6.78	Digital

*Prior to purchase/digitisation, each image was examined as a photographic print to ensure suitable coverage and sufficient image quality

Table 1: List of archive stereo-aerial photographs and their associated metadata for the field study sites Flower's Barrow and Eggardon hillforts.

The prints from BU and DCC were scanned using an A3 desktop scanner whilst the NMR scanned the requisite negatives using a Vexcel Photogrammetric Scanner. Each image was scanned at a resolution of 2400 dots-per-inch (dpi) and saved in the lossless TIFF file format. A recent set of commercially available, digital SAPs were obtained from GetMapping Ltd, created using a Vexcel UltraCamX digital aerial camera and delivered in JPEG format from the RGB (not panchromatic) sensors.

Archive airborne laser scanning (ALS) data from the EA was obtained for Flower's Barrow in its raw format to ensure that processing the data could be undertaken in a transparent way as the methods employed by the EA are not disclosed. A parallel dataset was not available for Eggardon.

2.3. Photogrammetric Processing

High-end photogrammetric software was chosen for processing archive SAPs, despite the popularity of Structure-from-motion (SfM) software with the archaeological community (Hullo et al. 2009; Ducke et al. 2011; Verhoeven 2011; Plets et al. 2012; Verhoeven et al. 2012a, 2012b; Koutsoudis et al. 2013; De Reu et al. 2013; Green et al. 2014; McCarthy 2014). Although SfM was initially considered as a means of processing archive SAPs, it was disregarded for its lack of optimisation for use with traditional, high resolution vertical stereo-aerial photographs. SfM is designed for use with lower-resolution photographs that are taken with a suggested overlap of +80% forward and 60% side (AgiSoft LLC 2014), not the 60% forward and 20-30% overlap present in SAPs. Whilst it is possible to obtain a DSM from SfM using archive SAPs, any metric information extracted from them should be examined carefully.

DSMs were created from SAPs using the SocetGXP® Automatic Terrain Extraction algorithm (ATE), the settings for which were determined via experimentation as described in Papworth (2014, p.153). SocetGXP® leads the user through a step-by-step workflow, prompting the input of interior and exterior orientation parameters. As with other such software packages, the best results are obtained if camera calibration data, namely fiducial coordinates, principle point location and lens distortion parameters are provided (Figure 6).

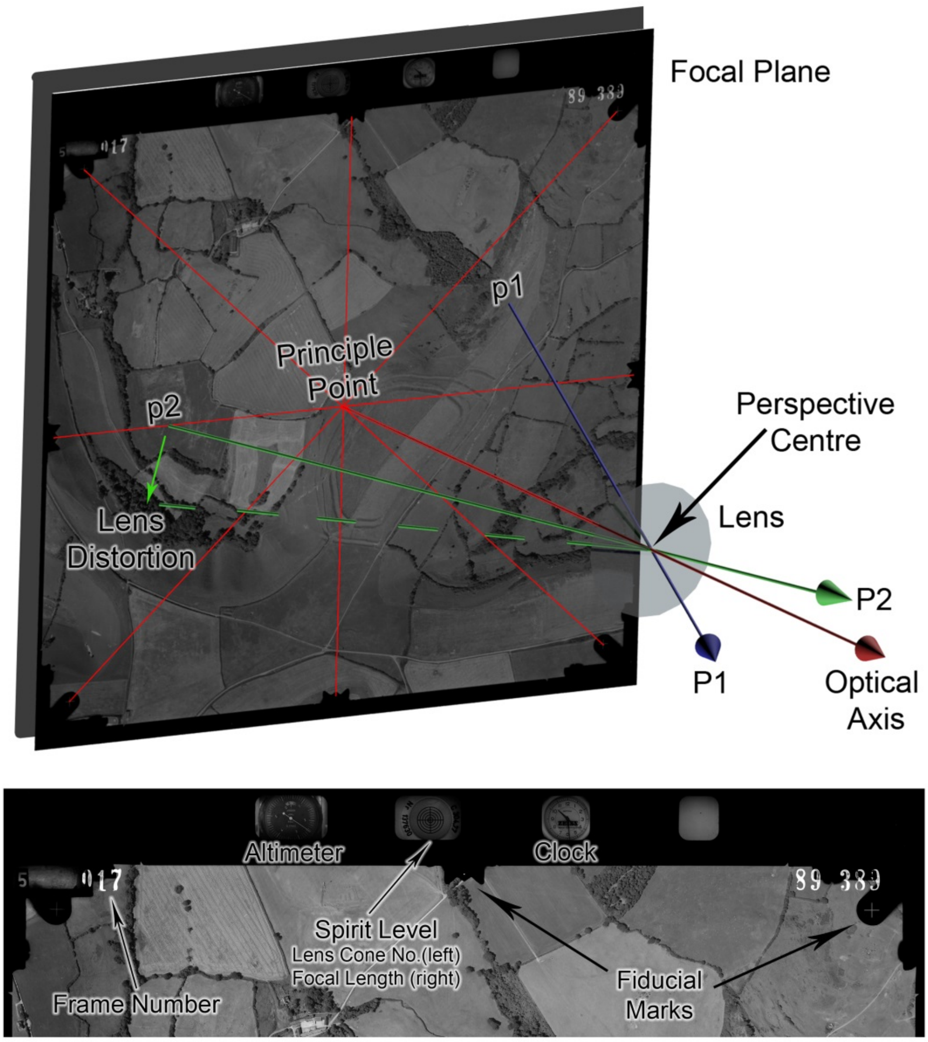

Figure 6: Diagram illustrating the components of interior orientation (top) and the information strip often provided with an aerial photograph (below) (Papworth 2014, p59).

However, many of these measures are not available for archive SAPs but, to account for these issues, the software includes a self-calibrating bundle adjustment routine. With the exception of the 2009 and 2010 SAPs from GetMapping

Ltd, which were provided with camera calibration and exterior orientation information, the remaining SAP datasets were processed using the self-calibrating bundle adjustment to obtain the missing camera parameters. To mitigate for the lack of interior orientation data and exterior orientation information (i.e. GNSS camera positions at the time of exposure and the associated rotation measures describing the attitude of the camera at this time) a large number of ground control points (GCPs) were collected (Figure 7). The GCPs were gathered as close to the point of interest (each hillfort) as possible. The objects used as GCPs were features identifiable in the archive SAPs such as gate

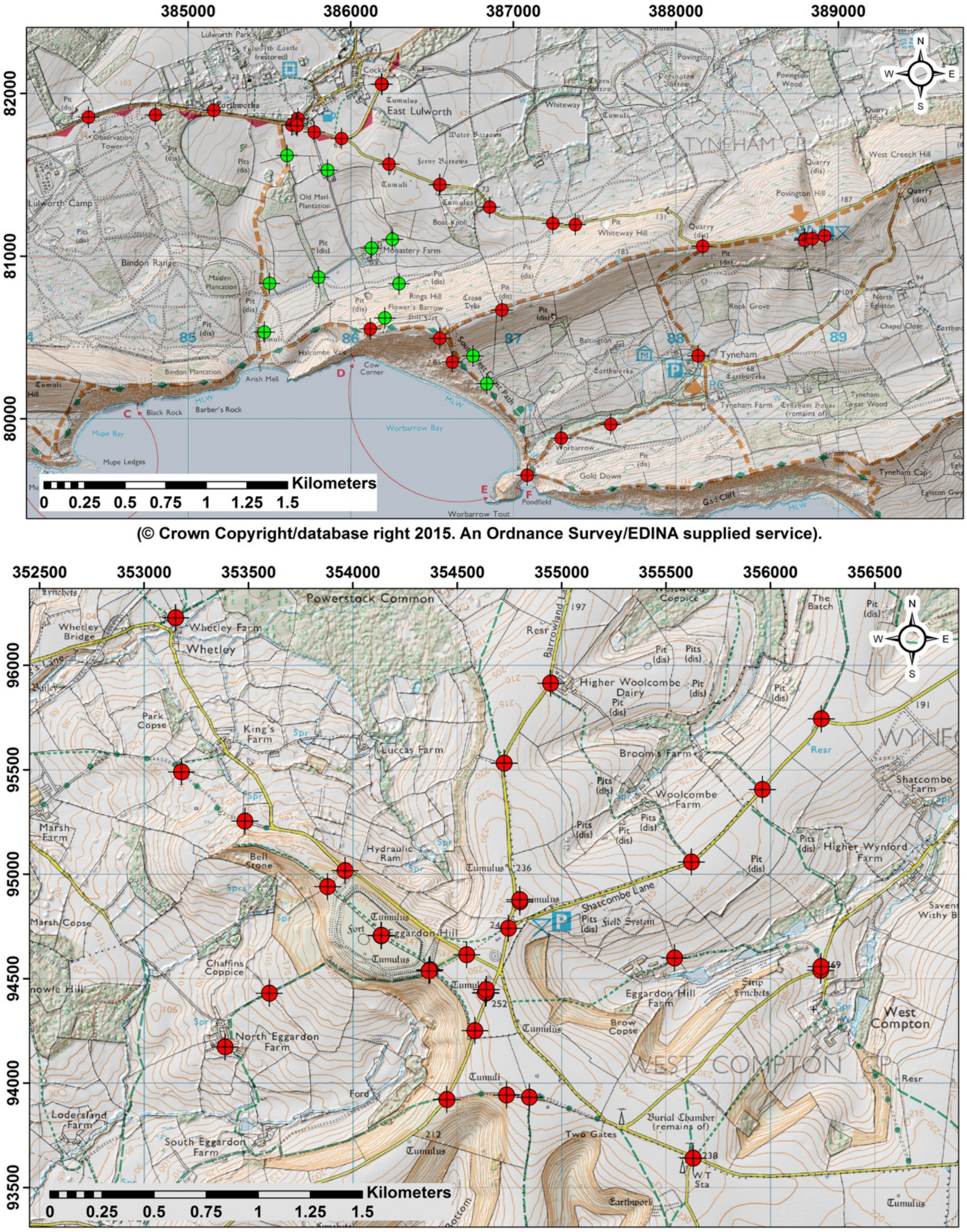

(© Crown Copyright/database right 2015. An Ordnance Survey/EDINA supplied service).

(© Crown Copyright/database right 2015. An Ordnance Survey/EDINA supplied service).

Figure 7: Location map showing the distribution of GNSS ground control points, shown in red, for (a.) Flower's Barrow (GCPs from alternative mapping sources shown in green) and (b.) Eggardon hillfort (Papworth 2014).

posts, road intersections, and the corner of structures such as buildings for example. Flower's Barrow proved challenging because of its location on a live firing range and the restricted access to the area surrounding the site. A large number of GCPs were recorded using a Leica Viva GNSS that, when operating in Network RTK mode (i.e. receives real-time positional corrections from static reference stations within the UK via a mobile phone), has a stated accuracy of 8mm horizontally (+0.5 parts per million, or ppm) and 15mm vertically (+0.5ppm) (Leica Geosystems AG, no date). However, many of the GCPs situated to the north of the hillfort within the fields and the farm area were extracted from 1:1000 scale Ordnance Survey mapping and a 3rd party 2m DSM. The fields and roads surrounding Eggardon were fully accessible, facilitating the collection of GCPs across the area of interest. Due to the problems encountered with the lack of mobile phone reception in the area, Network RTK was not available and thus GCPs were gathered using a Leica GS10 reference station in combination with the GS15 rover. This data was subsequently post-processed using Leica GeoOffice software, which resulted in a mean accuracy per GCP of 0.014m.

The workflow developed for this research utilised a small number of initial tie points to ensure an acceptable solution was achieved for relative orientation between the SAPs when the bundle adjustment was first run. The overall root mean square error (RMSE) was used to assess the orientation result, as it represents a global measure of the accuracy with which the software has calculated the solution for the relationship between the SAPs and the GCPs. A minimum RMSE value was sought by variously tightening and loosening the exterior orientation accuracy values, and removing tie points with the largest errors. Subsequently, more tie points were added along with a small number of GCPs. These were required to provide locational information in an appropriate coordinate system and strengthen the relationship between the images. As each GCP recorded with the Viva GNSS is stored with data quality information, it was possible to input these values into SocetGXP®, adding an extra 20cm to the x/y values, as suggested by Walstra et al (2011), to account for potential offsets caused by GNSS errors and the observer identifying GCP locations within the imagery.

The process was continued until no further decrease could be obtained in the root mean squared (RMS) value. The accuracies achieved during triangulation of the imagery are shown in Table 2. A DSM of 1m resolution was extracted from the data using the ATE adaptive algorithm and exported from SocetGXP® as a point cloud for interpolation in ArcMap 10.1. As these data were to be validated using independent DSM datasets, described in Section 2.4.1, standardising the interpolation algorithm used was necessary to limit the variables capable of influencing data quality and subsequently its analysis. The 'natural neighbour' interpolator was employed because it has been identified as an accurate method to apply to high resolution datasets (Abramov and McEwen 2004, Bater and Coops 2009) and is stated by Maune et al. (2007) to work well with both regular and irregularly-spaced point cloud data and is not prone to introducing artifacts.

	Flowers Barrow				
	Triangulation Root Mean Square Residuals				
Date Flown	**Image (Pixels)**	**X (m)**	**Y (m)**	**Z (m)**	**Total RMS (m)**
Mar 1945	8.333	3.592	2.440	4.480	5.915
Aug 1968	1.004	2.776	2.120	6.494	7.374
Apr 1982	1.518	1.588	1.783	2.204	3.142
Sept 2009	1.136	8.326	9.699	3.157	1.317

	Eggardon hillfort				
	Triangulation Root Mean Square Residuals				
Date Flown	**Image (Pixels)**	**X (m)**	**Y (m)**	**Z (m)**	**Total RMS (m)**
Jan/Mar 1948	3.198	2.807	1.244	5.220	5.791
Apr 1969	1.142	3.797	8.092	4.085	8.948
Oct 1972	6.564	2.115	1.744	1.138	2.969
Apr 1984	6.243	5.900	3.164	1.815	1.934
Jul 1989	6.385	3.758	5.879	2.670	7.471
Sept 1997	2.466	7.829	1.452	5.256	1.731
May 2010	6.675	7.325	7.668	2.428	1.088

Table 2: Results of the image triangulation process in SocetGXP®

2.4. Validation Methods

2.4.1. Quantitative Assessment

Objective assessment of error in the SAP DSMs was undertaken on their elevation values in comparison with those of the TLS collected at each field site (see Section 2.1). This was achieved by subtracting each of the SAP DSMs from the TLS DSM to create a DSM of Difference (DoD) for each SAP epoch that contained the residual values between terrain models. These values were extracted from each DoD to create a table of residual values that are taken from each cell of the raster, which in turn were used to create summary statistics as described in Section 2.4.2. The desktop scanned SAPs for Flower's Barrow were not assessed as the pilot study utilised only the NMR imagery to determine the viability of the research.

Error assessment was enhanced by converting the elevation DSMs from both the SAPs and the TLS into first-order derivatives, namely 'slope' and 'aspect', as per the approach advocated by Gallant and Wilson (2000). Whilst useful in their own right as terrain attributes, the conversion of elevation data into first-order derivatives can enhance noise or other errors contained in the original dataset, helping to identify problematic regions within a dataset. Therefore each of the SAP slope DSMs were subtracted from the TLS slope model to create a slope DoD, and the same process was repeated for the aspect datasets. The residual values from each of the slope and aspect DoDs were exported to SPSS for statistical analysis (Section 2.4.2).

2.4.2. Summary Statistics

A number of statistical measures were used to assess whether systematic or random errors were present in the SAP DSMs. Systematic errors are caused by a bias within the photogrammetric workflow, such as errors in pixel geometry of a sensor (camera or scanner), or lens distortion for example (Mitchell 2007). These errors can be mitigated if they have been measured, modelled and a correction for them applied (Wolf and Dewitt 2000). Random errors are sometimes referred to as noise and are related to data quality, although tend to be difficult to predict. Within the SAPs, these errors are caused by poor image geometry and image blur, for example, although other sources of random error, such as image resolution and scale can, to some extent, be predicted. In TLS data, random errors are caused by adverse influences on the laser beam, such as particulate matter in the air (i.e. water droplets), or strong winds destabilising the instrument during data collection for example. Systematic errors tend to be a consistent value (i.e. photographs taken with the same lens will all contain the same amount of lens distortion) and affect the accuracy of the data by shifting calculated values by a known quantity away from the 'true' value (the latter of which can never truly be determined). However, as systematic errors are consistent, they do not influence precision, which is related to the repeatability of measurements. Precision is influenced by random errors that do not have consistent values and are often difficult to account for.

Global indicators of DSM error, namely root mean square error (RMSE), mean error (ME) and standard deviation (SD), were calculated to objectively compare the TLS DSM to each SAP DSM (Baily et al. 2003, Walstra et al. 2004, Papasaika et al. 2008, Aguilar et al. 2009, Walstra et al. 2011, Perez Alvarez et al. 2013). RMSE was used as an indicator of accuracy and to identify the presence of systematic errors within the SAP DSMs (Dowman and Muller 2011), therefore the larger the RMSE error, the poorer the accuracy of a dataset in comparison with the baseline TLS. SD was used to indicate the precision of the SAP DSMs as this value is influenced by the presence of random errors in a dataset. ME values reveal bias (Fisher and Tate 2006), which can be introduced by systematic errors that cause under- or over-estimation of elevation values. With the exception of the RMSE, which was calculated in Microsoft Excel, both the ME and SD from each DoD were created using SPSS.

Frequency histograms of the residual values were generated from the data to determine whether the residual distribution between each SAP DSM and that of the TLS is normal. Such distributions are generally indicative of random errors, with increasing histogram width illustrating a decrease in precision. A skewed distribution, which contains the majority of residual values either in the left or right-hand section of the graph, may indicate the presence of systematic bias in a dataset. In this particular instance, camera calibration information detailing the lens distortion parameters, fiducial marks coordinates and the principle point were not available for any of the SAP datasets, with the exception of the 2009 and 2010 images for Flowers Barrow and Eggardon Hillfort respectively, and thus it was anticipated that the results would highlight the presence of systematic errors.

The peak of the distribution also provides an important indicator of difference. If all systematic errors were eliminated via the use of an appropriate photogrammetric model, only the remaining random errors would influence this peak. Subsequently, the size of these errors will be represented by the Kurtosis (spikiness) of the histogram.

Scatter plots were also created to identify whether a linear relationship exists between the SAP DSMs and the independent dataset, namely the TLS. This process plots the elevation values of one dataset against another and can reveal how similar or different these data are. A positive, linear relationship, or correlation, between the two datasets would indicate their similarity.

2.4.3 Spatial Autocorrelation of Errors

In addition to the absolute (global) indicators of error calculated above, local Moran's I analysis was undertaken to determine how errors were spatially distributed across a DSM. This was important as, although the DoDs for elevation, slope and aspect illustrate spatial distribution of residual values, they do not indicate whether these differences are statistically significant. The results generate a diagram indicating where, across the area of interest, clusters of statistically significant high (shown in red) or low (blue) residual values occur as well as regions with non-significant values (grey), an example is provided in Figure 8. Statistically significant values that are surrounded by either much lower (light blue) or higher (orange) values are indicative of outliers. Together, both the clusters and outliers are suggestive of values that exceed what would be expected from random error (ESRI 2014).

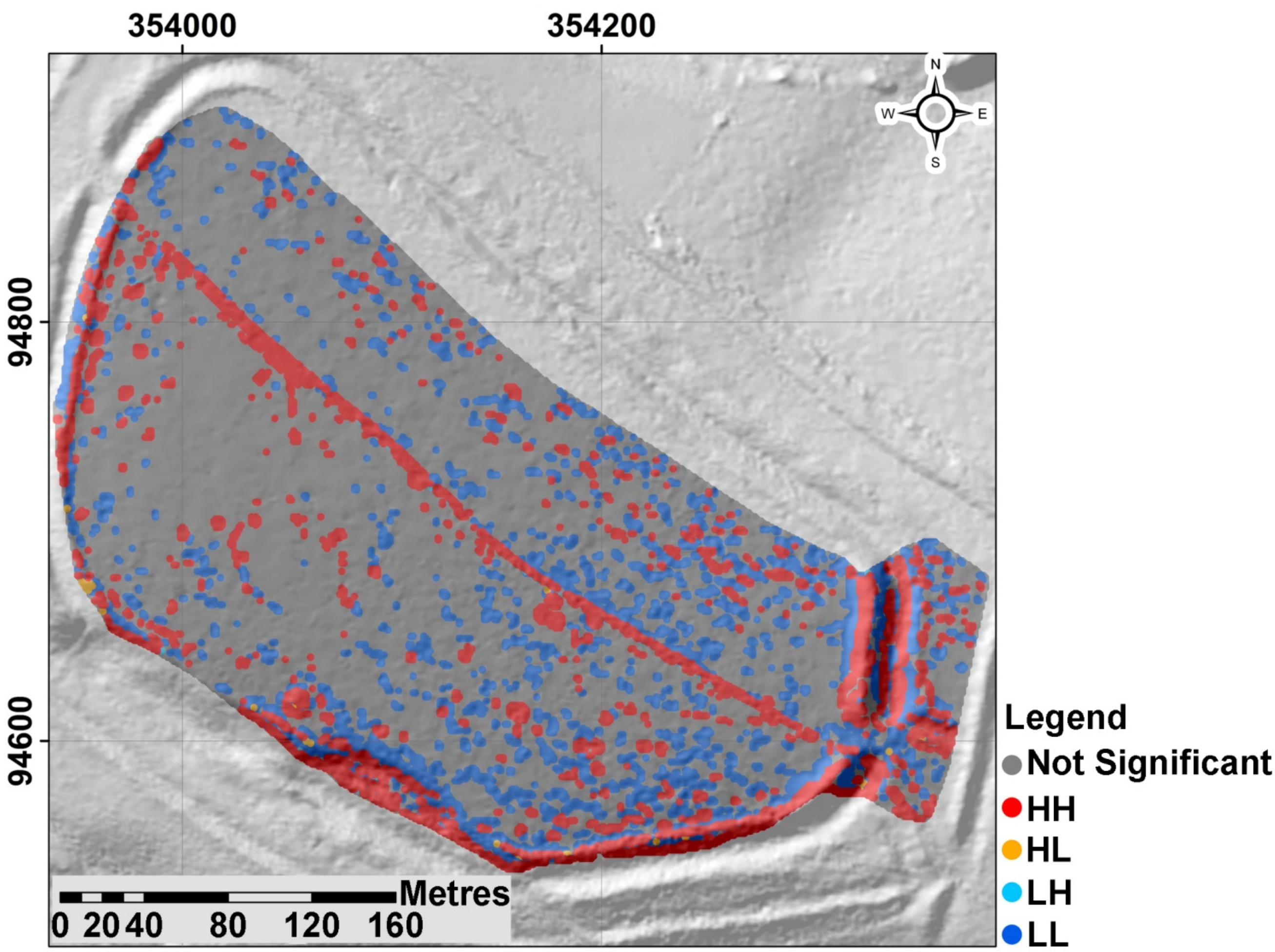

*HH=Statistically Significant High Value, HL=High Value Surrounded by Low Values, LH=Low Value Surrounded by High Values, LL= Statistically Significant Low Value. The significance level is set at 95%.

Figure 8: Example of a Moran's I diagram illustrating the statistical significance of residual slope values between the 1984 SAP data and that of the TLS across Eggardon.

2.4.4. Qualitative Assessment

In addition to the metric performance of each dataset, the SAP DSMs were assessed against the interpretive surveys produced by the Royal Commission for Historical Monuments of England (RCHME) for each site. Profile data were extracted from each SAP DSM epoch and their form compared to that of the profile lines recorded by the RCHME on their hachure plans from Eggardon (RCHME 1952) and Flower's Barrow (RCHME 1970). Point data were generated along the location of the profile line as shown on each hachure plan by importing the georeferenced RCHME data into ESRI ArcMap v10. These were then extracted to provide locational information for the GNSS, and the stakeout function used to locate the profile line in the field and re-measure it. This approach facilitated the direct comparison of profile data as captured during a conventional archaeological survey (RCHME) with that created by mass-capture and GNSS methods to assess how representative the latter were of archaeological earthworks.

3. Results

3.1 Quantitative Assessment of DSM Quality

3.1.1 Summary Statistics

The summary statistics from both Flower's Barrow and Eggardon, based on the comparison of SAP DSM elevation, slope and aspect values with those of the TLS data, are presented in Table 3. The general trend in the results supports the observation that DSM quality increases as SAP age decreases. This is illustrated by the decrease in ME, SD and RMSE values, although there are two important exceptions to this: the DSMs derived from the desktop scanned prints within the Eggardon dataset and the 2009 digital photography obtained for Flower's Barrow. The differences between these datasets and the others are more easily discernible by examining the slope and aspect results, which exhibit greater disparities due to the conversion of elevation values into first-order derivatives.

The residual histograms (Figures 9 and 10), display normal distributions for both field sites when comparing the slope and aspect differences between the SAP and TLS values.

		Flower's Barrow				
		TLS MINUS 1945	**TLS MINUS 1968**	**TLS MINUS 1982**	**TLS MINUS 2009**	**TLS MINUS 2009 ALS**
	Number of values	47361	51759	51759	51759	51759
Elevation	**Mean Error (m)**	0.035	-0.163	-0.126	-0.097	-0.399
	Std. Deviation (m)	1.204	0.741	0.213	0.619	0.394
	RMSE (m)	1.205	0.759	0.248	0.626	0.561
Slope	**Mean Error (degrees)**	-2.210	1.630	0.213	0.584	-0.582
	Std. Deviation (degrees)	8.914	8.250	3.532	7.830	6.059
	RMSE (degrees)	9.184	8.410	3.538	7.852	6.087
Aspect	**Mean Error (degrees)**	-5.278	3.949	-0.093	-0.354	-1.920
	Std. Deviation (degrees)	47.767	44.873	20.453	31.628	28.032
	RMSE (degrees)	48.057	45.046	20.453	31.629	28.097

		Eggardon hillfort						
		TLS Minus 1948	**TLS Minus 1969**	**TLS Minus 1972 (DTS)***	**TLS Minus 1984**	**TLS Minus 1989**	**TLS Minus 1997 (DTS)***	**TLS Minus 2010**
	Number of values	89021	89021	89021	89021	89021	89021	89021
Elevation	**Mean Error (m)**	0.172	-0.044	-0.145	-0.386	0.076	0.171	0.282
	Std. Deviation (m)	2.572	0.390	0.664	0.248	0.150	0.505	0.155
	RMSE (m)	2.577	0.392	0.6796	0.459	0.168	0.533	0.321
Slope	**Mean Error (degrees)**	-14.410	-1.171	-3.540	-0.666	0.191	-3.166	0.481
	Std. Deviation (degrees)	12.253	4.249	6.385	3.300	3.021	5.959	2.278
	RMSE (degrees)	18.915	4.408	7.301	3.366	3.027	6.748	2.328
Aspect	**Mean Error (degrees)**	-13.663	-4.581	-7.232	-1.202	-0.681	-7.487	1.569
	Std. Deviation (degrees)	68.852	52.521	61.173	48.557	44.069	62.097	39.191
	RMSE (degrees)	70.195	52.721	61.599	48.572	44.074	62.546	39.223

*DTS = Desktop Scanned Prints

Table 3: Summary statistics for Flower's Barrow (top) and Eggardon hillfort (below) showing the global errors between the TLS DSM and the SAP DSMs and their derivatives

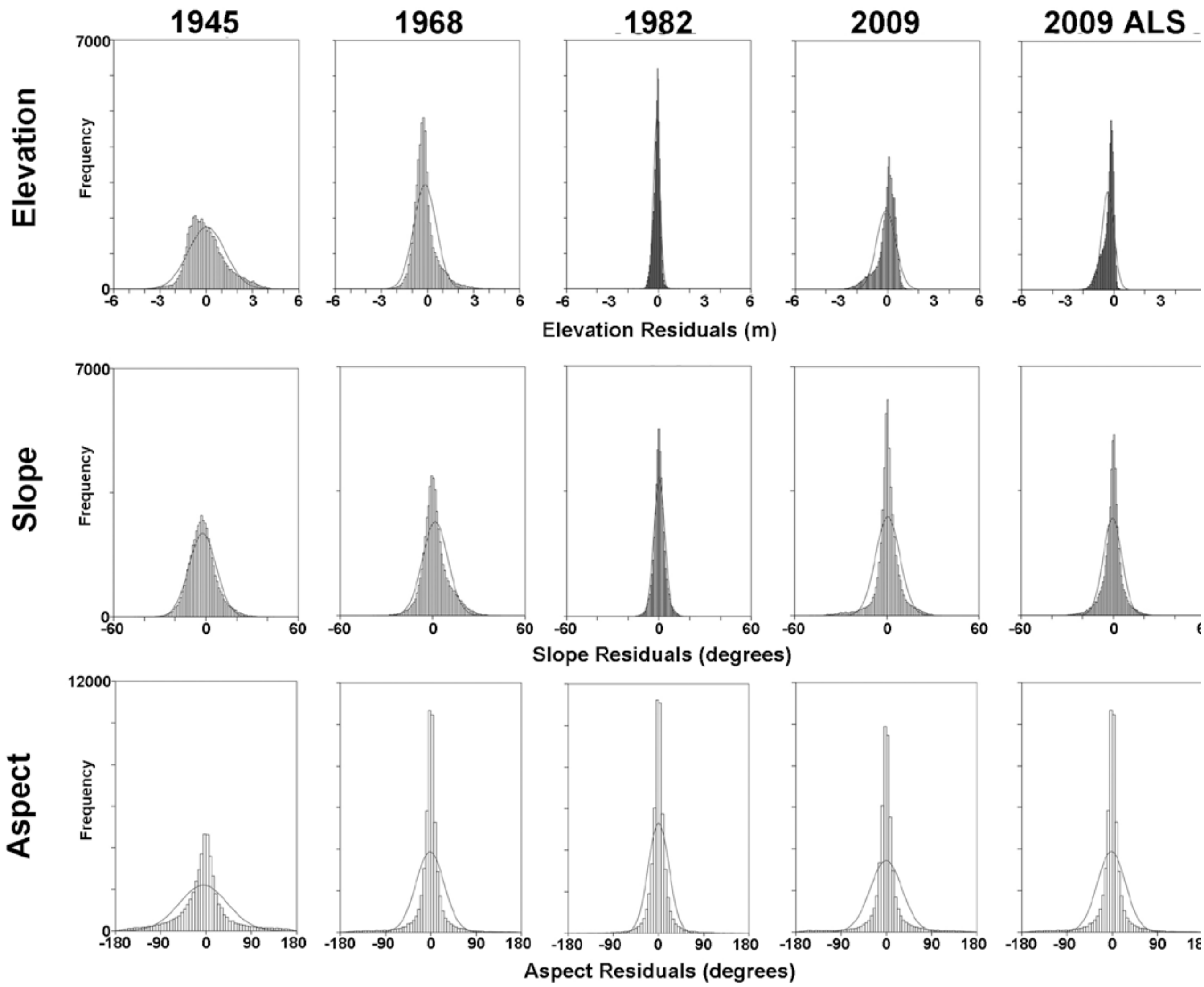

Figure 9: Residual Histograms of DSM difference for Flower's Barrow. The normal distribution is represented by the bell-shaped line.

The majority of the histograms are leptokurtic i.e. demonstrates a high peak. Greater variation in histogram shape was observed across the SAP DSM elevation values for both sites (Figures 9 and 10). The Flower's Barrow elevation residual histograms were positively skewed for the 1945 and 1968 SAPs whilst negatively skewed for the 2009 SAPs and the 2009 ALS data, with the latter exhibiting a more leptokurtic peak. The 1982 SAP residual histogram was, however, normally distributed and displayed a leptokurtic peak. Bimodal distributions were observed in the Eggardon elevation residuals for the 1948, 1972 and 2010 SAP DSMs, indicating the presence of two modes (i.e. there are two residual values that most commonly occur) within the data. The second, much smaller peak of residuals for the 1948 and 1972 datasets are comprised of negative values, whilst the second peak within the 2010 data has a very small spread but a leptokurtic peak that occurs around 0m. The remaining epochs, namely the 1969, 1984, 1989 and 1997 SAP DSM residual histograms, are all normally distributed with leptokurtic peaks.

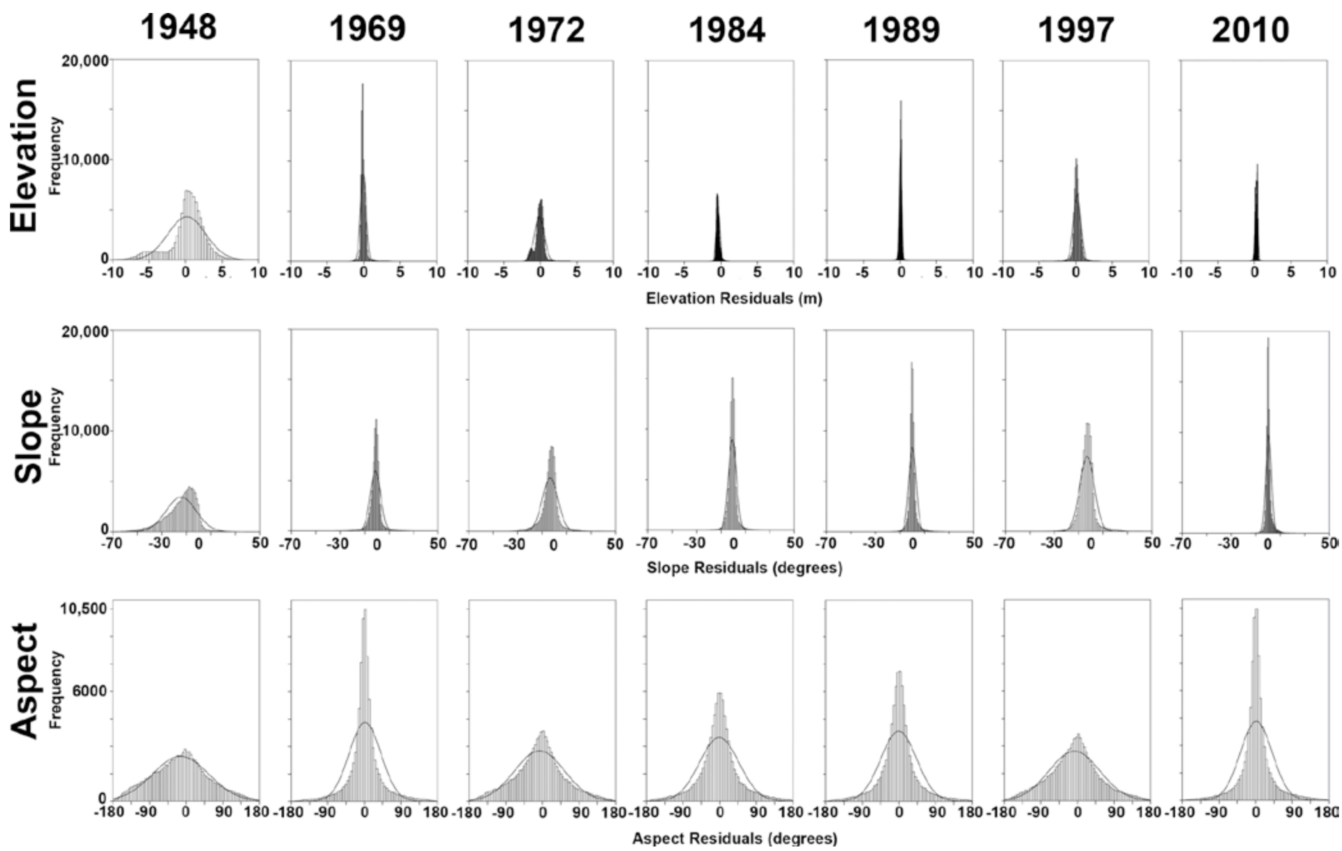

Figure 10: Residual Histograms of DSM difference for Eggardon. The normal distribution is represented by the bell-shaped line.

Scatter plot results for discerning the relationship between the SAP DSM elevations and the TLS DSM (Figure 11 and 12), generally increase in positive linearity as SAP age decreases for both sites, although there are a number of exceptions highlighted in the Eggardon dataset (Figure 12).

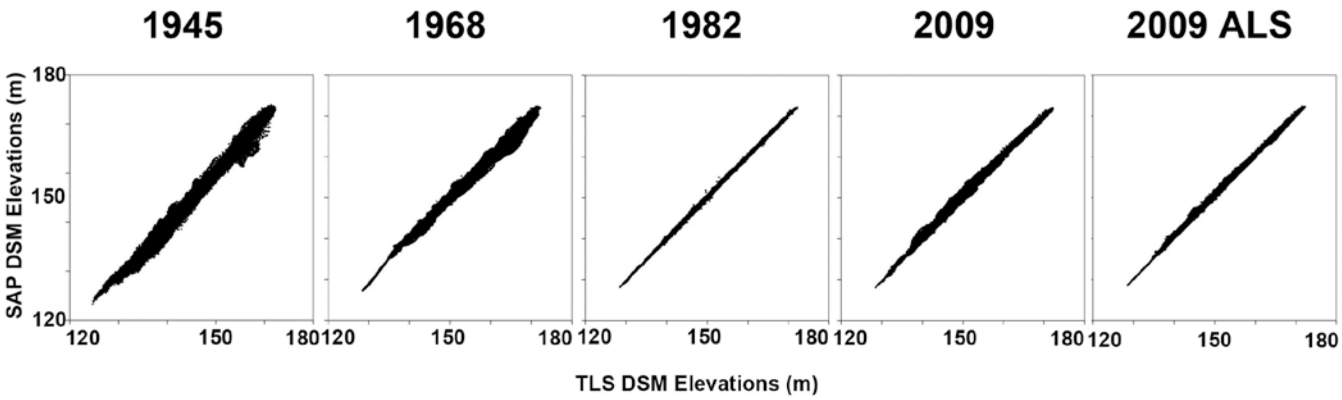

Figure 11: Flower's Barrow Elevation Scatter Plots

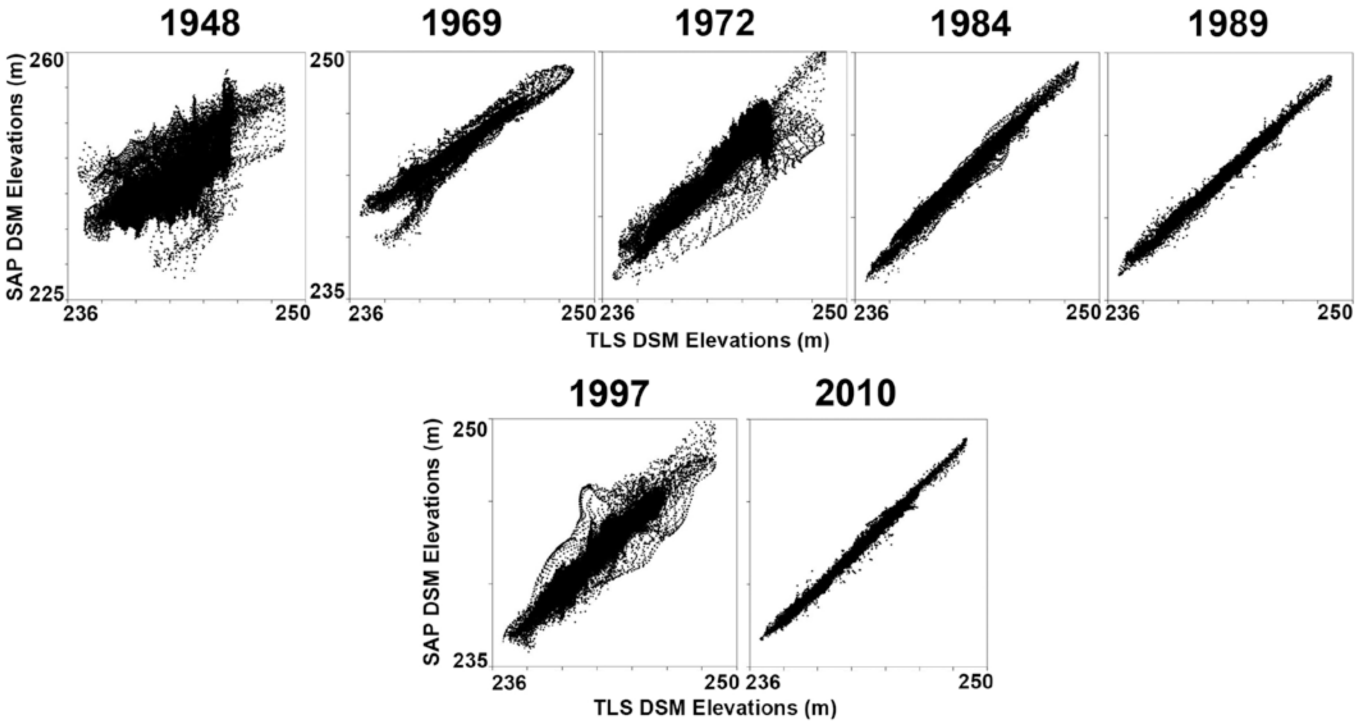

Figure 12: Eggardon Elevation Scatter Plots

The 1972 and 1997 Eggardon scatter plots (Figure 12), whilst broadly linear, contain a large amount of noise, as demonstrated by the spread of the values within the graph, which subsequently thickens the appearance of the linear scatter. However, this does not greatly affect their correlation values, as shown in Table 4, which contains Pearson's 'r' values, where any value from 0.5 to 1.0 indicates a high, positive correlation (Field 2013, p.82).

	Flower's Barrow Correlations			
	N*	**Elevation Correlation**	**Slope Correlation**	**Aspect Correlation**
TLS vs. 1945	47361	0.993	0.710	0.562
TLS vs. 1968	51759	0.997	0.700	0.595
TLS vs. 1982	51759	1.000	0.949	0.922
TLS vs. 2009 SAPs	51759	0.998	0.750	0.814
TLS vs. 2009 ALS	51759	0.999	0.856	0.856

	Eggardon hillfort Correlations			
	N*	**Elevation Correlation**	**Slope Correlation**	**Aspect Correlation**
TLS vs. 1948	89021	0.717	0.300	0.144
TLS vs. 1969	89021	0.981	0.725	0.510
TLS vs. 1972	89021	0.949	0.419	0.323
TLS vs. 1984	89021	0.992	0.832	0.572
TLS vs. 1989	89021	0.997	0.851	0.656
TLS vs. 1997	89021	0.967	0.423	0.308
TLS vs. 2010	89021	0.997	0.917	0.729

*N = number of elevation/slope/aspect values compared

Table 4: Pearson's 'r' correlation values obtained by comparing the TLS elevation and first-order derivative data to that of the SAPs at both Flower's Barrow and Eggardon hillfort.

The 1948 elevation results from Eggardon exhibit the least significant relationship with an 'r' value of 0.717, although this differs markedly to the results obtained for the 1945 SAPs at Flower's Barrow, which obtained a value of 0.993. It is also evident that, for the data at both field sites, the correlation between the TLS and SAP data decreases when converted to a first-order derivative (Table 4). These statistical data also indicate that correlation improves as the age of the SAPs decrease.

3.1.2 Spatial Autocorrelation of DSM Errors

The residual values from the elevation, slope and aspect Moran's I maps all demonstrate that the residual distribution is clustered for both sites, as illustrated in Figure 13 and 14.

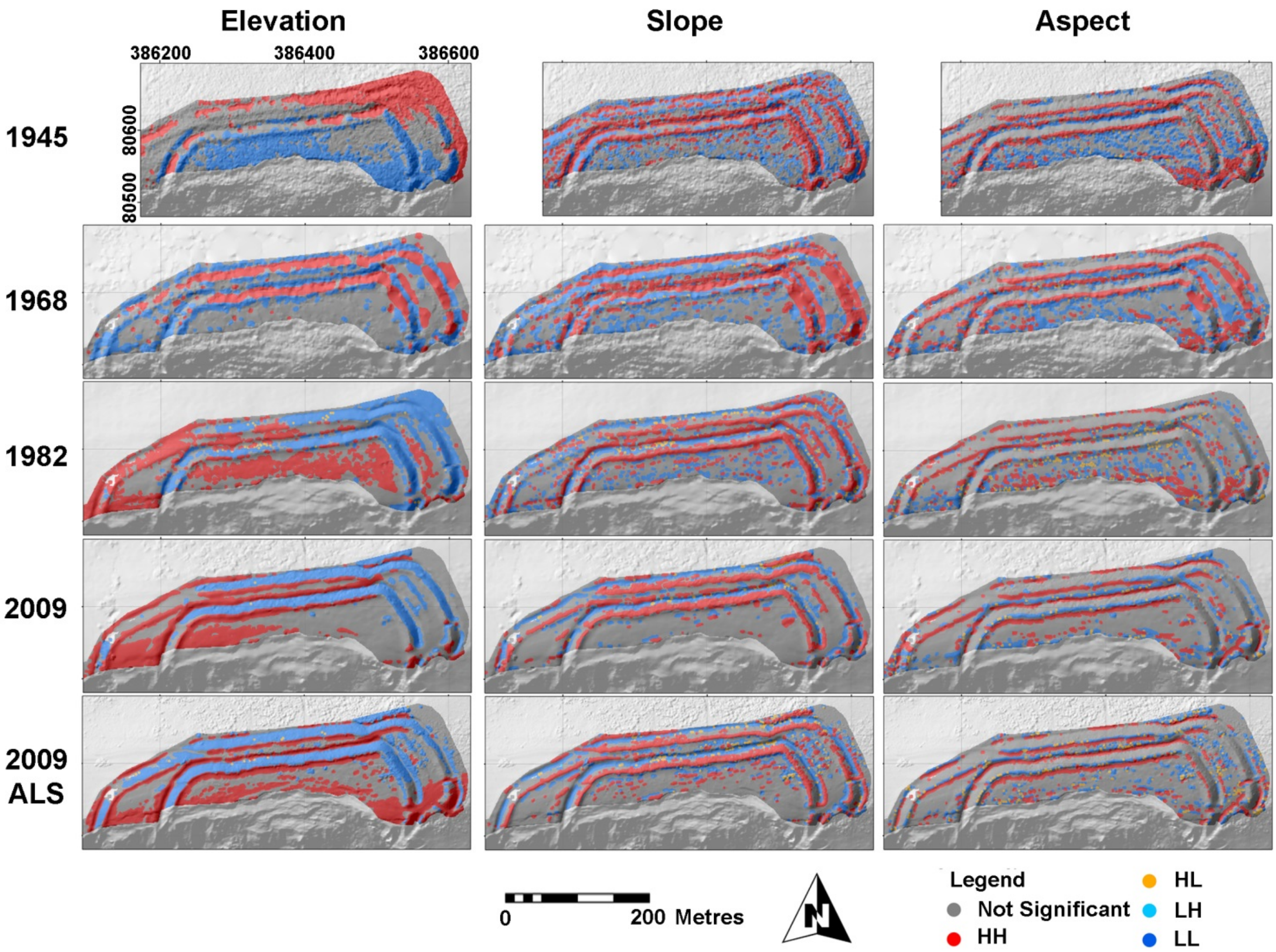

Figure 13: Flower's Barrow Local Moran's I Results

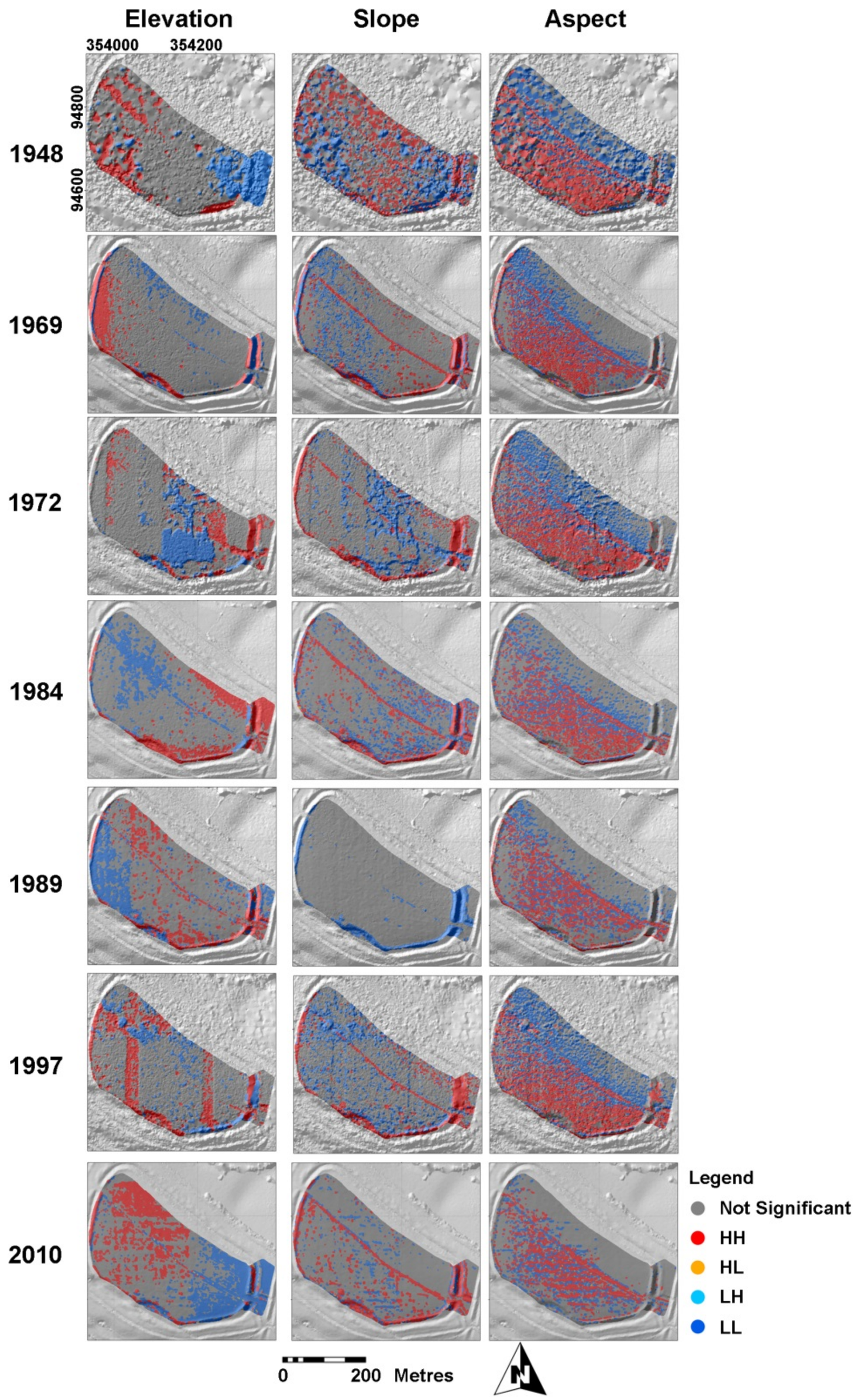

Figure 14: Eggardon Local Moran's I Results

An examination of the Flowers Barrow elevation datasets in Figure 13 indicates consistent clustering of values on the rampart slopes for each epoch, including the ALS, with the exception of 1945. Within this diagram there appears to be some distinction between clustered low values to the south-west and clustered high values to the north-east. This is suggestive of a systematic error in the photogrammetric model created from the 1945 SAPs which, at first glance, may indicate a tilt within the SAP DSM. However, if this were the case, it would be expected that a distinctive cluster of high values would be followed by an area of non-significant values where the pivot point of the tilt would be, which would then turn in to a region of low values. The pattern shown within the 1945 elevation Moran's I diagram may show large blocks of high and low values, but each is interspersed with clusters of values of the opposite sign. Subsequently, it is unlikely that tilting of the SAP DSM is the cause of this difference. This same pattern is not apparent in the slope and aspect derivatives from the 1945 DSM although, as derivative values of elevation, they are independent of the factors affecting a tilt in elevation models.

A pattern of high and low value clustering along the rampart slopes and in the ditches of Flowers Barrow can be identified in all of the Moran's I diagrams, with the exception of the 1945 elevation map. Based upon the quality assessment undertaken on the TLS data in Section 2.1.1 these errors are not caused by low point densities or accuracies in this dataset. Whilst the largest errors between the TLS and GNSS datasets were located along the inner most north-facing rampart slope, they do not occur sufficiently frequently elsewhere within the hillfort to suspect that deficiencies in the TLS data influence the pattern of spatial clustering within the Moran's I results. The pattern of clustering suggests that, as slope angle increases, so to do the differences between the TLS and SAP datasets.

Within the Eggardon Hillfort results, as shown in Figure 14, there are different patterns of clustering. Most notable within the elevation diagrams are the stripes of clustered values that are especially evident in the 1972 and 1997 DTS datasets. These stripes do not necessarily coincide with features in the imagery, such as the information strips, the edge of a frame or an artefact in the images themselves, although they have structure and are suggestive of a systematic error. As this pattern is noted in the two datasets scanned from prints using a desktop scanner it is likely that the source of error may be related to the use of print materials and an uncharacterised scanner, the issues of which are discussed in Section 4.3.

A further systematic error appears to be present in the 2010 elevation diagram as shown by the clustering of significant high values to the west and significant low values to the east. The transition between these significant values occurs on the boundary between coverage of 6 stereo pairs (west) and 4 stereo pairs (east) in the image block. It is possible that this difference in stereo coverage created differences in number and accuracy of tie points in the block adjustment and also a difference in the number of stereo-matched points in the cloud used to interpolate the DSM. Subsequently, this would result in different significant residuals across the DSM when compared with reference data. Were the block to be extended to create a consistent stereo coverage across the site, such that 6 stereo pairs covered the east of the hillfort, it is likely that these significant differences in residuals would be of the same sign, minimised, or absent.

As with the Flowers Barrow datasets, there are noticeable clusters of significant values along the rampart slopes of the hillfort in the majority of the elevation and slope diagrams for all SAP epochs. These are most pronounced along the slope of the east-facing rampart, situated to the east of the hillfort. As with the Flowers Barrow results, an examination of the TLS data density and accuracy in Section 2.1.1 does not depict any obvious deficit in the data which may influence the outcome of the Moran's I analysis. There is one exception to this observation and that is the line of high values running from the north-west to the south-east of the hillfort, which is synonymous with the fence that denotes the boundaries of ownership. This feature was not removed from the TLS dataset and thus indicates elevation values that are expected to be much higher than those contained within the SAP DSMs. Overall, these results support the same conclusion as Flowers Barrow, in that an increase in the slope angle of the ramparts decreases the accuracy of its representation in comparison with the TLS data.

3.2 Qualitative Assessment of DSM Data

The profiles illustrated in Figure 15 show that the results for Eggardon appear to create a more reliable reconstruction of the ramparts than those for Flower's Barrow. There is close conformity with the RCHME survey of Flower's Barrow from the GNSS with the exception of the plateau in the middle of the profile. Aside from the 1945 and 1968 DSMs the profiles from the remaining SAP DSMs are remarkably similar. The same can be said of the Eggardon profile whereby SAP data from 1969 onwards conforms to the RCHME survey. In corroboration with the quantitative results, the DSMs from newer SAPs create profiles that are more consistent with the shape of the rampart banks and ditches than those from the older photography and the images scanned from prints using a desktop scanner. Subsequently, it can be

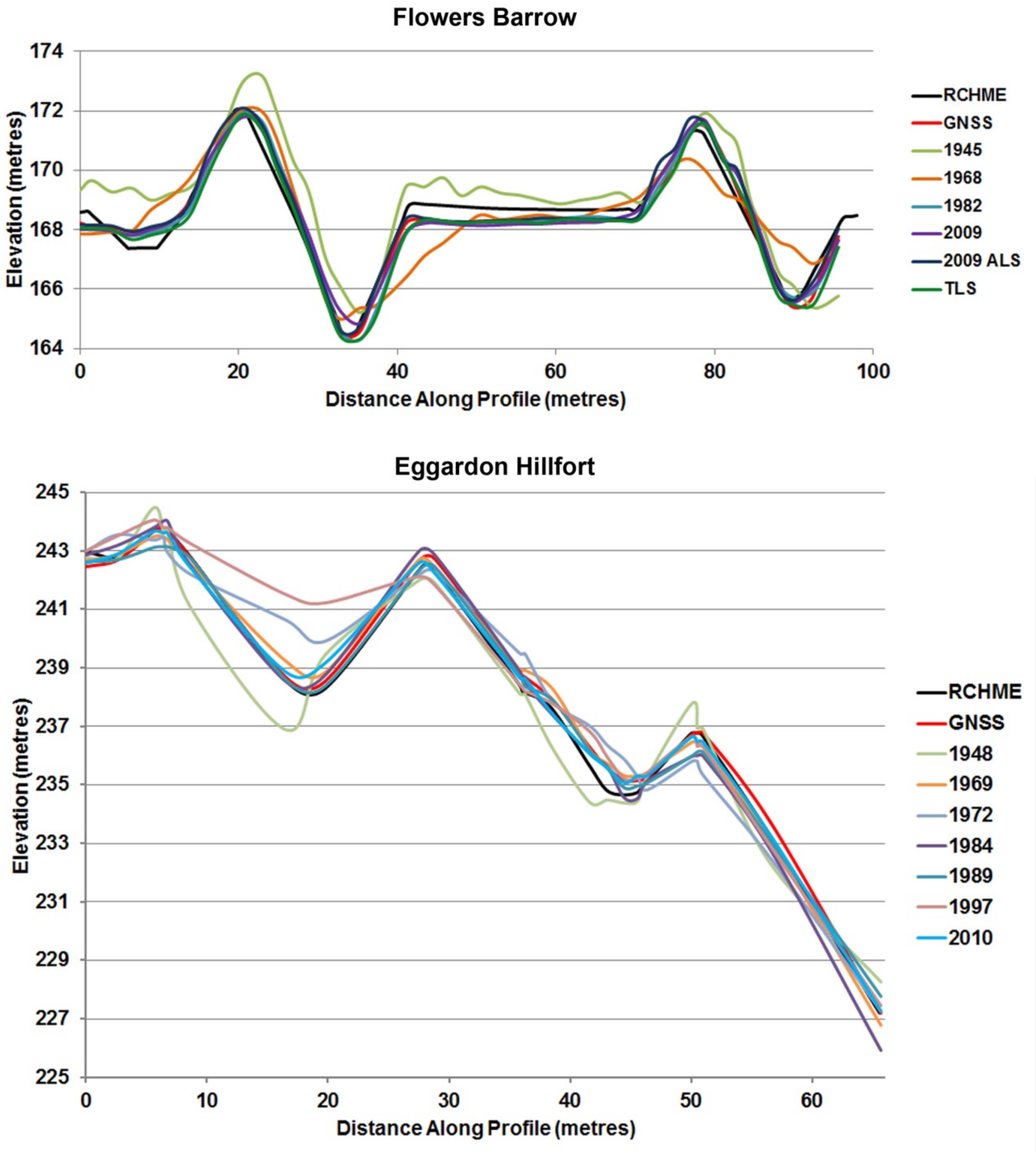

Figure 15: Profile Comparisons between the RCHME survey, GNSS and SAP DSM results.

said that SAP DSMs can be used to provide archaeological survey data, although photography from the 1940s and from desktop scanned photographic prints cannot.

4. Discussion

The results, both empirical and qualitative, demonstrate that archive SAPs can be used to generate data akin to that of the RCHME surveys whilst highlighting a number of issues that should be considered when undertaking DSM generation with these data.

4.1 SAP Age

It has been demonstrated that the quality of DSM output does generally improve with decreasing imagery age: a trend which has also been identified by previous studies conducted by Walstra et al. (2004) and Aguilar et al. (2012). Both authors provide tables showing a decrease in RMSE values as the age of SAPs also decrease. However the relationship is complex and influenced by a variety of factors such as camera and film quality, suitable GCPs and the state of preservation of photographic materials, for example.

The weakest performing DSMs were produced from the 1945 and 1948 photographs from Flower's Barrow and Eggardon respectively (see Section 3.1.1). The 1945 SAP DSM from Flower's Barrow is missing the western tip of the hillfort due to a lack of stereo-overlap in this region. However, when comparing the appearance of the 1945 and 1948 DSMs with one another (see Figure 13 and 14) the 1945 data has a less noisy appearance and the lack of stereo-overlap does not appear to have hindered reconstruction of the hillfort to the centre and east of the earthwork. This disparity between two SAP datasets of similar age illustrates the variation in image quality depending on location for the period 1945-'51. During this period the RAF were responsible for the acquisition of aerial photography over the United Kingdom on behalf of the OS. The cameras and aircraft used were not designed for photogrammetric use (Owen and Pilbeam 1992). For instance, the most widely employed cameras (F24 & F52) were non-metric, relatively small-format (5 x 5" and 8.5" x 7" respectively) and instead designed for aerial reconnaissance (Conyers Nesbit 2003). A minority of sorties were flown at relatively low altitude with comparatively short focal lengths (2133.6m and 8" over Flowers Barrow in 1945), but the majority, especially in rural areas, were flown at greater altitudes with longer focal lengths (5029.2m and 20" over Eggardon in 1948). The resulting photo scales were very similar (1:10500 and 1:10000 respectively) but with markedly different baseline-to-altitude ratios, with the latter making photogrammetry very difficult. These are the most likely explanations for the differences in photogrammetric results between 1945 and 1948 presented here.

These problems were further exacerbated by the use of "split-vertical" camera pairs. In the case of the Spitfire PR XIX, as used over Eggardon in 1948, this arrangement had two F52 cameras angled 5° 20" from the vertical (Evidence in Camera, March 1945). This resulted in low-oblique photographs, with twice the coverage of a single camera. This was ideal for aerial reconnaissance but came at the expense of photogrammetry. With few photogrammetric plotters available (Whitaker 2014) the emphasis was instead on the creation of photo-mosaics for reconstruction purposes. The RAF were also unable to guarantee a supply of aircrew experienced in aerial survey, given problems of recruitment and retention (Macdonald 1992).

From 1951 the OS resumed control of aerial photography acquisition, but aircraft and aircrew were provided by the Ministry of Transport & Civil Aviation, who proved unsatisfactory for similar reasons as the RAF. For the majority of the 1950s and early 1960s aerial survey was limited in quantity and extent (Macdonald 1992) and thus archival photography was not available for either Flowers Barrow or Eggardon.

It was only after the purchase of 9 x 9” format metric cameras (i.e. Zeiss RMK 30/23 & Wild RC8R) and the use of civilian contractors for flying that matters finally improved from the mid-1960s (Survey Season, in FLIGHT International, 4th January 1965. p. 49 & 50). Stricter quality-control requirements stipulating the timing and weather conditions (including sun angle) were also used by the OS and contractors. Therefore DSMs from SAPs dating from the mid-1960s onwards for both sites do not demonstrate as stark a difference as the data from the 1940s.

Further developments saw the RAF re-equipped with the Canberra PR 3, 7 & 9 aircraft and, whilst still employing split-vertical pairs of F52, they also carried the F49 9 x 9” format survey camera (Oakey 2008). These resulted in superior photogrammetric products, as demonstrated with the SAP acquired over Flowers Barrow in 1968.

Based on the reasons stated above the authors recommend that archive SAPs of the UK dating from the 1945-‘65 period require independent consideration and verification, especially those acquired from 1945-’51.

In the 1980s the OS purchased cameras with forward motion compensation (i.e. Zeiss RMK 15/23 & Wild RC10A/RC20), which further improved photogrammetric products (Macdonald 1992). However, it is arguable that the introduction of colour film at the OS and commercial companies, in part to meet the growing requirement for colour orthophotographs, may have negatively impacted photogrammetry in terms of the lower granularity with greater film density (the opposite of black & white films) (Langford 1998).

4.2 Image Resolution

In comparison with the analogue archive SAPs, the most recent 2009 digital photography generated over Flower’s Barrow by GetMapping Ltd. did not perform as favourably as the ALS and 1982 SAP datasets. This is illustrated by the summary (global) statistics provided in Table 3. The elevation data from the 2010 digital photography of Eggardon was also out-performed by 1989 OS SAPs on comparison of the RMSE values, which are 0.321m and 0.168m respectively. The cause of this is postulated to be the reduced detail captured by the digital multispectral camera system of the Vexcel UltraCam X from which the images were provided (unfortunately, the panchromatic images were not available in the scope of this project). Unlike the 6µm pixel size of its panchromatic camera, the multispectral imagery delivers a pixel size of 18µm (Microsoft Corp. 2008), providing an image with pixel dimensions of 5770x3770 pixels and a ground-sample distance (GSD) of 0.15m. Therefore, the newest SAP datasets for both field sites have the lowest GSD of the group and contains a lesser amount of information per pixel than the film-based imagery of earlier sorties.

It should be noted that image resolution for scanned photographs is dependent on the abilities of the scanner used to digitise them. Whilst much of the issues surrounding scanners and the effect of photographic materials on resolution will be discussed in Section 4.3, a brief appraisal of scan resolutions is given here. Walstra et al. (2011) state that a scanned pixel size of 6 to 12µm would be required to preserve a resolution of 30 to 60 lines/mm as provided by original film, based on a paper by Baltsavias (1999) who states that good DSM results can be acquired when using a scan resolution of 25-30µm. The photographs for this research were scanned at a resolution of 2400 dots-per-inch or 10.6µm whilst those utilised by Walstra et al. (2011) and Aguilar et al. (2013) range between 15 - 42 µm. However, the increased resolution of the scanned images used in this research will not necessarily increase the precision of the resultant DSMs if the original film quality, atmospheric conditions at exposure and processing methods, for example, are such that image quality is already degraded prior to scanning. Aguilar et al. (*ibid.*) compared the overall RMSE results obtained from 1977 imagery, , with values obtained by Walstra et al. (2007) for 1971 (1.31m).

A further consideration regarding the GetMapping imagery is the provision of such in the compressed jpeg file format, as was the case for this research, and whether this may have had a negative impact on DSM quality. Lam et al. (2001) have shown that utilising jpeg files with a compression ratio of less than 10 should have no significant impact upon DSM quality, unless the image is texturally rich. If so, there will be a more significant degradation of image quality, which in turn affects the quality of the resultant DSM. As no information relating to the compression ratio was provided with the GetMapping data for this research, the adverse influence of jpeg compression on the DSMs created using this imagery cannot be dismissed.

4.3 Photographic Materials and Scanning Technologies

The positive influence of the use of well-defined photogrammetric scanning technology upon archive SAPs can be seen by examining the Eggardon dataset. Tables 2 and 3 demonstrate the overall weak performance of the 1972 and 1997 SAP DSMs. This disparity is due to the scanning of these images using commercially available desktop equipment that had not been characterised to provide error correction factors for any geometric or radiometric distortions it may introduce to the digitised photography. Geometric errors (i.e. lens distortion, defective pixels and CCD misalignments) and radiometric errors (i.e. illumination instabilities, stripes and electronic noise) are rarely, if ever, accounted for by manufacturers of desktop scanners (Baltsavias and Waegli 1996; El-Ashmawy 2014), with the radiometric errors in particular varying on a frequent basis (Baltsavias and Waegli *ibid.*), thus illustrating the instability of this equipment. El-Ashmawy (*ibid.*) states that photogrammetric scanners are manufactured to robust standards to ensure the accuracy of analogue to digital image production at every stage of the scanning process, which also illustrates the inflated cost of these scanners.

All other SAPs from this site were scanned from original negatives using a photogrammetric scanner (see Section 2.2), and the DSMs produced from this imagery performed well. The 1948 SAPs form the only exception to this result producing data seen to be inferior to both the 1972 and 1997 SAPs. Here age is thought likely to be the dominant factor (see Section 4.1). A comparative study on the influence of scanning technologies upon archive SAPs and the extraction of DSMs using SfM software has been investigated by Sevara (2013). The author also concluded that DSMs obtained using photography scanned from negatives contained less distortion and performed better than scans obtained from print materials. Print materials produce photographs with lower detail due to the larger size of silver crystals used in their emulsions, as compared to that used in film (Walstra et al. 2011), and are known to be more susceptible to degradations (Jacobson 2000, p373). Degradations can take a variety of forms such as image fading and staining (caused by residual chemicals in photographic material or oxidisation of silver particles by atmospheric gases, for example) or microbial attack on the gelatin contained with a negative or print, and on the paper substrate within print materials. High humidity will cause gelatin in photographic materials to swell that, in a photographic print, can also encourage some of the layers to detach, particularly around the edges, which gives rise to this ‘frilling’ as well as blistering on the print surface (Weaver 2008, p13). Weaver (*ibid.*, p14) also highlights further issues with humidity, namely ‘cockling’ of print materials, which can occur differentially across a photograph as the gelatin and paper expand at different rates, and the reduction of paper flexibility that enhances the likelihood of tearing and cracking in this substrate. These factors highlight the challenges in removing geometric distortions from archive photographs, particularly from prints.

Overall, the results from this section of our study reflect the findings from Walstra et al. (*ibid.*) in that the values obtained from scanned prints are worse than those from scanned negatives. Walstra et al. (*ibid.*) state that the accuracy values from scanned prints may be worse by a factor of 3.1 in comparison with scanned diapositives, although the authors also note that this value is based upon limited data. It should also be remarked that different photogrammetric software, namely Leica Photogrammetry Suite (LPS), was utilised by this study and thus the results from an alternative package, such as SocetGXP, may be different. However, it is nevertheless a useful indication of the quality of data achievable when utilising poorer-quality data.

4.4 Control and Tie Point Distribution

The distribution of tie points and GCPs across each set of imagery is suspected to be the cause of bimodal distributions observed in the elevation residual histograms obtained for the 1948, 1972 and 2010 Eggardon datasets. A lack of sufficient control close to the edges of the photographs, where lens distortion is at its peak, may cause the triangulation routine to perform sub-optimally. Triangulation utilises both tie points and GCPs to calculate missing exterior orientation and camera calibration information, including the lens distortion parameters. Subsequently, image matching in these regions may perform sub-optimally, particularly if radial distortion has been modelled poorly, and the triangulation solution may result in values that increase with distance from the principle point. This issue will propagate into the terrain extraction process whereby unrepresentative elevation values may appear in areas where the SAPs overlap, causing artifacts to appear in the DSM. These were observed in the 1972, 1997 and 2010 Eggardon DSMs, manifesting as a stripe effect running north-south through the hillfort (Figure 11). However, the 1997 residual histogram does not display a bimodal distribution, which may suggest that the elevation offsets in the SAP DSM caused by the stripe may be negated by the other elevation values within the data.

Studies by Walstra (2006) and Aguilar et al. (2012) have referred to optimal GCP numbers when processing archive SAPs, with Walstra (*ibid.*) using between 4 to 9 per stereopair and Aguilar et al. (*ibid.*) identifying similar triangulation accuracies irrespective of whether 12 or 24 GCPs were utilised. Subsequently, the latter research recommended the use of 6 to 9 GCPs per stereopair (14 when using very old photographs of lower geometric and radiometric quality and/or smaller scale) if self-calibrating bundle adjustment was required, as was the requirement for this project due to the deficit of camera calibration data. However, as Walstra et al. (2011) note, selecting suitable control in historical imagery is often limited, relying instead on site accessibility and/or change since the photography was captured and must thus be considered based upon the features visible in any one image set. Subsequently, the number of GCPs identified per stereopair, per epoch for this research were akin to those used by Walstra (2006), namely between 4 to 9 GCPs. It should also be noted that a number of natural features (i.e. fence and gate posts, road intersections) were used as GCP locations, which have been identified by Walstra et al. (2011) as a potentially large source of uncertainty, particularly when compared with artificial targets deployed as a control network during contemporary a photogrammetric survey.

4.5 Camera Calibration Information

Camera calibration information was only available for the most recent digital photography, namely the 2009 Flower's Barrow and 2010 Eggardon datasets from GetMapping Ltd. However, this did not appear to influence the quality of the DSM results, particularly for the Flower's Barrow field site over which the 1982 SAP DSM performed most favourably in comparison with the TLS, as highlighted by the summary statistics provided in Table 3. In addition, the inclusion of camera calibration information for the 2009 and 2010 digital photography did not prevent the clustering of residual values (Table 4). These results suggest that calibration information does not greatly influence the occurrence of systematic errors. Therefore, whilst it is good practice to work with camera calibration information where possible, for archival imagery their absence should not significantly negatively impact on the result obtained.

4.6 Archaeological Implications

The recording of archaeological earthworks, particularly those at threat from attrition, should be regularly recorded for management and monitoring purposes (ICOMOS General Assembly 1996). Metric information is crucial for these purposes, playing an important role in the analytical process of understanding a monument and mapping changes that are occurring or may occur in due course. However, as demonstrated by the field sites utilised for this study, the only known survey data of each consists of an interpretive hachure plan and selected profiles, which depict the form of the earthworks but do not facilitate future mapping and monitoring practices. Subsequently, the regaining of metric data for such purposes in relation to these sites is only possible via the use of SAPs. This research has demonstrated that many of the photogrammetrically scanned SAPs and the DSMs created from them have been able to provide metric information akin to that recorded using a TLS. This has been demonstrated by high correlation values between the elevation data produced by photogrammetry and laser scanning. It has also been shown that profiles similar to the RCHME interpretive surveys can be extracted from SAP DSMs, thus illustrating the capability to extract archaeological information from archive SAPs.

5. Conclusion

In conclusion, this research has demonstrated that archive SAPs can produce data of archaeological utility. Archaeologists wishing to extract DSMs from these data are advised to consider a number of factors when pursuing their own SAP datasets. Firstly, SAP age influences DSM quality, with photography from the 1940s generating poorer results than DSMs generated using desktop scanned prints. However, the 1945 SAPs processed for Flower's Barrow did show promise, particularly when reconstructing the rampart slopes as illustrated by its profile. The digitisation method was also a key factor in producing high-quality DSMs and thus obtaining digital images scanned from negatives using a photogrammetric scanner will provide the best results.

Modern aerial photography providers should be asked to provide data from the panchromatic sensors in their digital cameras in a lossless (i.e. TIF format) as the RGB imagery processed by this research provided results that were, in the case of the Flower's Barrow study, poorer than imagery captured in 1982. Whilst camera calibration information did not appear to greatly influence the quality of the DSM results, GCPs should be gathered using GNSS equipment and, if possible, well distributed across the area of interest and throughout the photographic pair, strip or block.

The results presented by this research demonstrate that archaeologists must not solely rely on empirical analysis to assess DSM quality, but continue to conduct visual assessments of the data. This approach has been advocated previously by the archaeological community with reference to ALS DSMs (Doneus et al. 2008; Corns and Shaw 2009).

The implications the success of this method has upon archaeological research management and the mitigation of earthwork loss is significant. It provides a means by which to recover metric information lost through attrition, particularly if no prior record has been created. The reconstruction of larger earthworks has been demonstrated, and further work is required to assess this method for smaller earthwork features, such as pits and housing platforms.

6. Acknowledgements

This research was supported by a doctoral research studentship jointly funded by Bournemouth University (BU) and the National Trust. The authors would like to thank the technical staff at BAE Systems UK (Rick Mort, Steve Foster and Rut Gallmeier) for their help and advice regarding photogrammetric workflows and Professor Stuart Robson and Dietmar Backes (University College London) for training and assistance with SocetGXP. Thanks are also due to Martin Schaefer (University of Portsmouth) for initially providing photogrammetric scans of BU imagery and members of staff at the National Trust (Dr Martin Papworth, Guy Salkeld and Alison Lane) for providing help and access to National Trust resources. Grateful thanks are also extended to the two anonymous reviewers who took the time and trouble to make valuable comments and suggestions regarding the content of this paper.

7. References

Abramov, O. and McEwen, A. 2004. An evaluation of interpolation methods for Mars Orbiter Laser Altimeter (MOLA) data. *International Journal of Remote Sensing*, 25(3), 669-676.

Adams, J. and Chandler, J., 2002. Evaluation of Lidar and Medium Scale Photogrammetry for Detecting Soft-Cliff Coastal Change. *The Photogrammetric Record*, 17 (99), 405-418.

AgiSoft LLC, 2014. *Agisoft PhotoScan User Manual: Professional Edition, Version 1.1*. AgiSoft LLC.

Aguilar, M., Aguilar, F. and Negreiros, J., 2009. Self-Calibration Methods for Using Historical Aerial Photographs with Photogrammetric Purposes. *In: Ingegraf XXI* Lugo.

Aguilar, M. A., Aguilar, F. J., Fernández, I. and Mills, J. P., 2013. Accuracy Assessment of Commercial Self-Calibrating Bundle Adjustment Routines Applied to Archival Aerial Photography. *The Photogrammetric Record*, 28 (141), 96-114.

Baily, B., Collier, P., Farres, P., Inkpen, R. and Pearson, A., 2003. Comparative assessment of analytical and digital photogrammetric methods in the construction of DSMs of geomorphological forms. *Earth Surface Processes and Landforms*, 28 (3), 307-320.

Baltsavias, E.P., Waegli, B., 1996: Quality Analysis and Calibration of DTP Scanners. Paper presented at the 18th ISPRS Congress in Vienna. In 'International Archives of Photogrammetry and Remote Sensing', Vol. XXXI/B1, pp. 13-19.

Baltsavias EP. 1999. On the performance of photogrammetric scanners. *Photogrammetric Week* '99: 155–173.

Barber, M., 2011. *A History of Aerial Photography and Archaeology: Mata Hari's glass eye and other stories*. Swindon: English Heritage.

Bassegoda-Nonell, J., Benavente, L., Boskovic, D., Daifuku, H., Flores, C., Gazzola, P., Langberg, H., Lemaire, R., Matteucci, M., Merlet, J., Pane, R., Pavel, S. C. J., Philippot, P., Pimentel, V., Plenderleith, H., Redig de Campos, D., Sonnier, J., Sorlin, F., Stikas, E., Tripp, G., de Vrieze, P. L., Zachwatovicz, J. and Zbiss, M. S., 1964. The Venice Charter. In ICOMOS (Ed.). Venice.

Bater, C. W. and Coops, N. C., 2009. Evaluating error associated with lidar-derived DSM interpolation. *Computers and Geosciences*, 35 (2), 289-300.

Blake, B., 2014. The slippery slope: CAD hachures. *billboyheritagesurvey*. 13th March. Available from: http://wp.me/pYvo7-1ZR [Accessed 14th March 2014]

Bowden, M. and McOmish, D., 2012. A British Tradition? Mapping the Archaeological Landscape. *Landscapes*, 12 (2), 20-40.

Chandler, J., 1989. *The Acquisition of Spatial Data from Archival Photographs and Their Application to Geomorphology.* (PhD). City University, London.

Conyers Nesbit, R. 2003. *Eyes of the RAF: A History of Photo-reconnaissance*. Stroud: Sutton Publishing Ltd.

Darvill, T. and Fulton, A., 1998. *Monuments at Risk Survey 1995*. Bournemouth and London: Bournemouth University and English Heritage.

De Reu, J., Plets, G., Verhoeven, G., De Smedt, P., Bats, M., Cherretté, B., De Maeyer, W., Deconynck, J., Herremans, D., Laloo, P., Van Meirvenne, M. and De Clercq, W., 2013. Towards a three-dimensional cost-effective registration of the archaeological heritage. *Journal of Archaeological Science*, 40 (2), 1108-1121.

Dowman, I.J. and Muller, J.P. 2011. *Evaluation of Spaceborne DSMs: A Guide to Methodology*. Committee on Earth Observation Satellites, Terrain Mapping Subgroup.

Ducke, B., Score, D. and Reeves, J., 2011. Multiview 3D reconstruction of the archaeological site at Weymouth from image series. *Computers & Graphics*, 35 (2), 375-382.

ESRI, 2014. ArcGIS 10.1 Desktop Help. Cluster and Outlier Analysis (Anselin Local Moran's I) (Spatial Statistics).

Field, A. 2013. *Discovering Statistics Using IBM SPSS Statistics*. London: Sage.

Fisher, P. F. and Tate, N. J., 2006. Causes and consequences of error in digital elevation models. *Progress in Physical Geography*, 30 (4), 467-489.

Gallant, J. C. and Wilson, J. P., 2000. Primary Topographic Attributes. *In:* Wilson, J. P., and Gallant, J. C., eds. *Terrain Analysis. Principles and Practice.* John Wiley & Sons Inc.

Green, S., Bevan, A. and Shapland, M., 2014. A comparative assessment of structure from motion methods for archaeological research. *Journal of Archaeological Science*, 46 (0), 173-181.

Hullo, F., Grussenmeyer, P. and Fares, S., 2009. Photogrammetry and dense stereo matching approach applied to the documentation of the cultural heritage site of Kilwa (Saudi Arabia*). International Archives of Photogrammetry, Remote Sensing and Spatial Information Sciences*, XXXVIII-3.

ICOMOS General Assembly, 1996. *Principles for the Recording of Monuments, Groups of Buildings and Sites*, Sofia, Bulgaria 5-9 October.

Jacobson, R.E., 2000. Life expectancy of imaging media. In: Jacobson, R. E., Ray, S. F., Attridge, G. G. and Axford, N., eds. *The Manual of Photography*. Ninth Edition. Focal Press.

Koutsoudis, A., Vidmar, B. and Arnaoutoglou, F., 2013. Performance evaluation of a multi-image 3D reconstruction software on a low-feature artefact. *Journal of Archaeological Science*, 40 (12), 4450-4456.

Lam, K. W. K., Li, Z. and Yuan, X., 2001. Effects of JPEG compression on the accuracy of digital terrain models automatically derived from digital aerial images. *Photogrammetric Record*, 17(98): 331–342.

Langford, M. 1998. Advanced Photography, 6th Ed. Focal Press.

Leica Geosystems AG (no date). *Leica Viva GS15 Data Sheet* [online]. Available from: http://www.leica-geosystems.co.uk/downloads123/zz/gpsgis/Viva%20GS15/brochures-datasheet/Leica_Viva_GS15_DS_en.pdf [Accessed: 22nd November 2015].

Macdonald, A.S. 1992. Air Photography at the Ordnance Survey from 1919 to 1991. *The Photogrammetric Record*. 14(80): 249-260

Maune, D. F., Kopp, S. M., Crawford, C. A. and Zervas, C. E., 2007. Introduction. *In:* Maune, D. F., ed. *Digital Elevation Model Technologies and Applications: The DSM Users Manual, 2nd Edition.* Bethesda, Maryland: The American Society for Photogrammetry and Remote Sensing.

McCarthy, J., 2014. Multi-image photogrammetry as a practical tool for cultural heritage survey and community engagement. *Journal of Archaeological Science*, 43 (0), 175-185.

Miller, P., Mills, J., Edwards, S., Bryan, P., Marsh, S., Mitchell, H. and Hobbs, P., 2008. A robust surface matching technique for coastal geohazard assessment and management. *ISPRS Journal of Photogrammetry and Remote Sensing*, 63 (5), 529-542.

Mitchell, H., 2007. Fundamentals of photogrammetry. *In:* Fryer, J., Mitchell, H., and Chandler, J., eds. *Applications of 3D Measurement from Images.* Caithness, Scotland: Whittles Publishing.

Murphy, P., Thackray, D. and Wilson, E., 2009. Coastal Heritage and Climate Change in England: Assessing Threats and Priorities. *Conservation and Management of Archaeological Sites*, 11 (1), 9-15.

Oakey, T. 2008. Candid Canberra. *Aeroplane Monthly*. 36(2): 34-38

Odle, J. E. 1965. The Williamson F49 Mark 4 Air Survey Camera. *The Photogrammetric Record*. 5 (25): 37–49

Owen, T. and Pilbeam, E., 1992. *Ordnance Survey: map makers to Britain since 1791*. HMSO: London.

Oxford Archaeology, 2002. *Management of Archaeological Sites in Arable Landscapes*. London: DEFRA.

Papasaika, H., Poli, D. and Baltsavias, E., 2008. A Framework for the Fusion of Digital Elevation Models. *In: XXI ISPRS Conference "Silk Road for Information From Imagery"* Beijing, China.

Papworth, H., 2014. *An assessment of archive stereo-aerial photographs for 3-dimensional reconstruction of damaged and destroyed archaeological earthworks* [online]. (PhD). Bournemouth University. Available from: http://eprints.bournemouth.ac.uk/21780/ [Accessed: 6th January 2016].

Pérez Álvarez, J. A., Herrera, V. M., Martínez del Pozo, J. Á. and de Tena, M. T., 2013. Multi-temporal archaeological analyses of alluvial landscapes using the photogrammetric restitution of historical flights: a case study of Medellin (Badajoz, Spain). *Journal of Archaeological Science*, 40 (1), 349-364.

Plets, G., Verhoeven, G., Cheremisin, D., Plets, R., Bourgeois, J., Stichelbaut, B., Gheyle, W. and De Reu, J., 2012. The Deteriorating Preservation of the Altai Rock Art: Assessing Three-Dimensional Image-Based Modelling in Rock Art Research and Management. Rock Art Research, 29 (2), 139-156.

Royal Commission on Historic Monuments, 1970. An Inventory of the Historical Monuments of the County of Dorset: Volume II, South-East Part 3.

Royal Commission on Historical Monuments, 1952. An Inventory of the Historical Monuments in Dorset: Volume I, West Part 1.

Rowley, T. and Wood, J., 2008. *Deserted Villages*. Shire Publications Ltd.

Sevara, C., 2013. Top Secret Topographies: Recovering Two and Three-Dimensional Archaeological Information from Historic Reconnaissance Datasets Using Image-Based Modelling Techniques. *International Journal of Heritage in the Digital Era*, 2 (3), 395-418.

Walstra, J., Chandler, J. H., Dixon, N. and Dijkstra, T. A., 2004. Time for change - quantifying landslide evolution using historical aerial photographs and modern photogrammetric methods. In: *Proceedings of the 20th ISPRS Congress*. Istanbul, Turkey, 12-23 July 2004.

Walstra, J., 2006. *Historical Aerial Photographs and Digital Photogrammetry for Landslide Assessment.* (PhD). Loughborough University.

Walstra, J., Chandler, J. H., Dixon, N. and Wackrow, R., 2011. Evaluation of the controls affecting the quality of spatial data derived from historical aerial photographs. *Earth Surface Processes and Landforms*, 36 (7), 853-863.

Wessex Archaeology, 2001. Lulworth Ranges, South Dorset. Archaeological Integrated Land Management Plan (ILMP) Baseline Study. Desk-Based Archaeological Assessment and Monument Condition Survey.

Whitaker, K.A. 2014. The Wild Heerbrugg A5 in Britain in 2014. *The Photogrammetric Record*. 29(148): 456–462

Wilson, D. R., 2000. *Air Photo Interpretation for Archaeologists*. Stroud: Tempus Publishing Ltd.

Wolf, P. R. and Dewitt, B. A., 2000. *Elements of Photogrammetry: with Applications in GIS*. 3rd. Boston, USA and London, UK: McGraw-Hill.

Verhoeven, G., 2011. Taking computer vision aloft – archaeological three-dimensional reconstructions from aerial photographs with photoscan. *Archaeological Prospection*, 18 (1), 67-73.

Verhoeven, G., Doneus, M., Briese, C. and Vermeulen, F., 2012a. Mapping by matching: a computer vision-based approach to fast and accurate georeferencing of archaeological aerial photographs. *Journal of Archaeological Science*, 39 (7), 2060-2070.

Verhoeven, G., Taelman, D. and Vermeulen, F., 2012b. Computer Vision-Based Orthophoto Mapping of Complex Archaeological Sites: The Ancient Quarry of Pitaranha (Portugal-Spain). *Archaeometry*, 54 (6), 1114-1129.